SLAC-PUB-2700
PEP-NOTE-346
March 1981
(A)

EXPERIMENTAL OBSERVATIONS AND THEORETICAL MODELS FOR BEAM-BEAM PHENOMENA*

S. Kheifets
Stanford Linear Accelerator Center
Stanford University, Stanford, California 94305

"It is impossible to grasp a boundlessness.... "

....Kosma Prutkov†

Invited talk presented at the Workshop on Long-Time Prediction in Nonlinear Conservative Dynamical Systems
Austin, Texas
March 16 - 19, 1981

*Work supported by the Department of Energy, contract DE-AC03-76SF00515.
†The nickname for a Russian humorist collective author of the Nineteenth Century (A. Tolstoi, Two Brothers Zhemchuzhinikov).

1. INTRODUCTION:

PHENOMENOLOGY OF THE BEAM-BEAM INTERACTION

The beam-beam interaction in storage rings exibits all the characteristics of nonintegrable dynamical systems. Here one finds all kinds of resonances, closed orbits, stable and unstable fixed points, stochastic layers, chaotic behavior, diffusion, etc. The storage ring itself being an expensive device nevertheless while constructed and put into operation presents a good opportunity of experimentally studying the long-time behavior of both conservative (proton machines) and nonconservative (electron machines) dynamical systems — the number of bunch-bunch interactions routinely reaches values of $10^{10} - 10^{11}$ and could be increased by decreasing the beam current. At the same time the beam-beam interaction puts practical limits for the yield of the storage ring. This phenomena not only determines the designed value of main storage ring parameters (luminosity, space charge parameters, beam current), but also in fact prevents many of the existing storage rings from achieving designed parameters. Hence, the problem has great practical importance along with its enormous theoretical interest.

I present in this work a brief overview of the problem. Experimental observations, including the last available results from the PEP storage ring, will be discussed here together with the different theoretical and computational models suggested for understanding of the beam-beam phenomena. For the sake of completeness as well as to make the subject interesting for a person unfamiliar with the vocabulary and details of the field, I start with very informal description of a single particle motion in a storage ring. Then purely qualitatively the

electromagnetic force, which the particle of one bunch sees from the side of the other bunch, will be discussed. The dynamics of a particle in the presence of this force is described.

The rest of the introduction contains the phenomenological description of the beam-beam phenomena as it is seen by a machine physicist.

The bibliography on the subject includes hundreds of titles and is far beyond the space and time I have. A few references which one finds here are given only for the use of a reader who wants to go deeper into the field. Some of them depict certainly the most recent work performed on the beam-beam phenomena. The review of some work done in the past one can find in books[1,2] and in references.[3-5]

Illustrated (courtesy of Mr. B. Gould) is the present state of the entire beam-beam problem.

RACE TO THE BEAM LIMIT

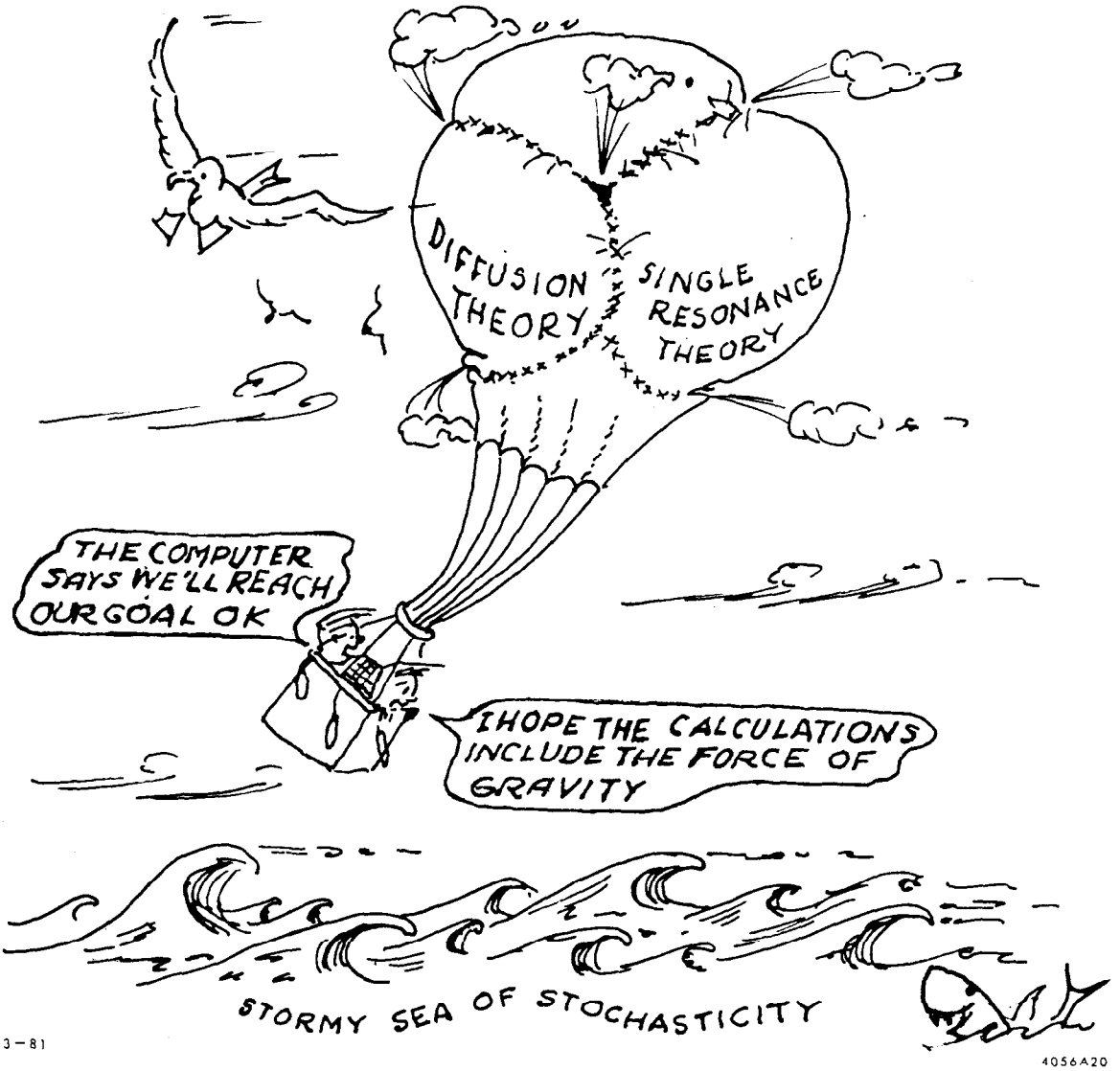

3-81

4056A20

1.1 One-Beam Single Particle Dynamics

In this section I will discuss a single particle motion in an electron storage ring with only one beam. The picture for a proton storage ring can be obtained from here by neglecting all the radiation effects.

An electron in the storage ring performs rather complicated motion which in the first approximation can be decomposed into three coupled oscillations — a longitudinal one called synchrotron oscillation and two transverse oscillations. In the limit of no coupling the last can be split into horizontal and vertical betatron oscillations, correspondingly. All three oscillations are nonlinear — the longitudinal one due to the sinusoidal form of high-frequency electric force, acting on a particle, and the transverse ones due to the presence of special sextupole magnets included in the lattice to control the chromaticity of the ring.* The frequency of oscillation is dependent on the particle amplitude A. The value of the frequency in the limit $A \to 0$ is called linear frequency. The ratio of the linear frequency to the revolution frequency is called the tune. Usually the longitudinal tune ν_s is much less than one (typically 0.05); that is, a particle performs one longitudinal oscillation in many revolutions. The tunes of betatron oscillations ν_x and ν_y are much bigger than one (for PEP they are around 21 - 23, i.e., a particle performs more than twenty betatron oscillations in one revolution).

In strong focusing machines (all the storage rings are such machines) the motion is described in terms of two proper functions of

*There are also other sources of nonlinearities (such as imperfections of the fields, collective fields, etc.) but the important point is that the motion is strictly speaking nonlinear even in an ideal machine.

the lattice: amplitude function (β-function) and dispersion function, to which a closed orbit for the particle with displaced momentum is proportional.

From the general condition for appearance of a resonance in the particle motion

$$m_x\nu_x + m_y\nu_y + m_s\nu_s = m \quad , \tag{1.1}$$

where m_x, m_y, m_s, m are any integers, we can ascertain the most dangerous resonances provided the force dependence on coordinate is known. For example, the most dangerous resonances exited by the sextupole field, for which the effective potential behaves like $x^3 - xy^2$, are

$$3\nu_x = m \tag{1.2}$$

$$\nu_x \pm 2\nu_y = m \quad . \tag{1.3}$$

The motion of a particle close enough to the origin is little effected by a nonlinear resonance. The phase trajectory of a particle is only slightly perturbed, staying essentially almost circular around the origin. At large distances from the origin, phase trajectory becomes completely different. In the picture of the Poincaré section appear additional fixed points. Each such point corresponds to a stable or unstable orbit, which closes on itself after a number of particle revolutions. Stable fixed points are surrounded by areas of stable motion, which are spearated from unstable fixed points by separatrixes ("islands").

The coupling of the longitudinal and transverse motions causes appearance of side lines near each linear and nonlinear resonance [term with ν_s in equation (1.1)]. Actual source of such coupling can be quite different: dependence of the tune on energy,[6,7] finite dispersion

function at an accelerating (or any other) cavity,[67] dependence of transverse amplitude on energy,[68] or transverse fields with longitudinal gradient.[8]

Due to finite site of a "good" field region, as well as due to nonlinear character of oscillations, not all amplitudes of the particle oscillations are stable. If an amplitude exceeds certain limits, the displacement of the particle from the equilibrium orbit will grow steadily and such particle will be lost from the beam. The maximum stable transverse amplitude determines the acceptance of the machine (for each plane).

An initial distribution of particles in phase space does not necessarily keep the same for the future times. There are many reasons for diffusion of the particle amplitudes towards bigger values. For electron storage rings the main source of the diffusion is quantum fluctuations of the radiation in the magnetic field. Other effects—intrabeam scattering of particles on each other, scattering on the residual atoms in the vacuum chamber, Arnold diffusion, noises in the power supplies, and so on—usually give smaller effects, but are important for a proton ring.

The diffusion processes of any kind would (and really do in proton machines) bring unlimited growth of the oscillation amplitudes and consequently lead to particle losses. Fortunately, at least for electron rings, there exists a mechanism of damping of the oscillations due to radiation friction. Two competing effects—quantum excitation and radiation damping—tend to balance each other, determining the equilibrium size of the bunch. This equilibrium is achieved in a time interval of the order of magnitude of the damping time and is independent of the

initial particle distribution. Typical damping time is of the order of 10^3 revolution periods. The equilibrium distribution function is unknown for nonlinear machines. For linear machines this distribution is Gaussian in all three degrees of freedom.

Although the radiation damping helps to limit rms amplitudes, presence of tails in distribution function makes the lifetime of the bunch finite. Particles are slowly but steadily lost from the bunch due to diffusion of a small portion of them toward the boundary of the machine aperture.

One of the intriguing possibilities for study of the emergence, development and limits of stochasticity is by measuring bunch lifetime for one beam operation mode of a storage ring with controlled nonlinearity.

1.2 Two-Beams Single Particle Dynamics

The presence in the machine of the second counterrotating beam exhibits significant influence on the dynamics of a particle. Collective electric and magnetic forces of the counterrotating bunch have the same direction and add together, giving in all formulae the additional factor $1+\beta^2$, where β is the relative velocity of the particle. The same forces of the bunch to which the particle belongs have the opposite directions and subtract, giving an additional factor $1-\beta^2 = 1/\gamma^2$. Hence, the force which a particle sees from an oncoming bunch is $\simeq 2\gamma^2$ times larger than the force from the other particles in the same bunch. In ultrarelativistic machines the latter effect is negligibly small.

The coordinate dependence of this force is determined by the geometry and the charge density distribution of the bunch. If the length of

the bunch is small enough (compared to the wave length of particle oscillations) and the charge density is not too large, then the particle does not change its displacement considerably during the interactions. In this case the particle experiences delta-function-like change in its transverse momenta, the magnitude of which are functions of its transverse displacements x and y at the interaction point.

For the three-Gaussian bunch "the kicks" $\Delta x'$ in horizontal and $\Delta y'$ in vertical directions can be found from the corresponding potential function in the following integral form:[9]

$$\Delta x' = - G(x/a) \int_0^1 d\tau \; e^{-\tau Q(x,y)} \left[p + \tau(1-p)\right]^{-3/2} \qquad (1.4)$$

$$\Delta y' = - G(y/b) \int_0^1 d\tau \; e^{-\tau Q(x,y)} \left[p + \tau(1-p)\right]^{-1/2} \qquad (1.5)$$

where

$$Q(x,y) = (y/b)^2 + (x/a)^2 \left[p + \tau(1-p)\right]^{-1} \qquad (1.6)$$

$$G = 2r_0 N / a\gamma \quad , \qquad (1.7)$$

r_0 is the classic electron radius ($\approx 2.82 \times 10^{-13}$ cm), N is the number of particles in thebunch, a and b are horizontal and vertical dispersions of the Gaussian distribution ($a = \sqrt{2}\,\sigma_x$, $b = \sqrt{2}\,\sigma_y$), and $p = b^2/a^2$ is aspect ratio of the bunch. The signs in (1.4,1.5) are chosen to describe an attractive force. They should be reversed for a repulsive one.

The most striking reatures of the force (1.4,1.5) are its nonlinear character and additional coupling it produces in particle motion. The force is linear only for very small values of y/b and x/b where the

charge is distributed more or less uniformly. It reaches maximum at the intermediate values of x/a. At very large distances from the origin the force falls off as $1/\sqrt{x^2+y^2}$. Figs. 1.1-1.6 illustrate the kicks $\Delta x'$ and $\Delta y'$ as functions of x/a and y/b for the round (p = 1) and for elliptical bunch cross section (p = 0.25).

For very small values of x/a << 1 and y/b << 1 Eqs. (1.4, 1.5) give:

$$\Delta x' = - Gx \Big/ \left(\sigma_x + \sigma_y\right) \qquad (1.4')$$

$$\Delta y' = - Gy \Big/ \left(\sigma_x + \sigma_y\right) \quad . \qquad (1.5')$$

In this approximation beam-beam interaction is linear and decoupled. The action of the opposite bunch can be described as an additional thin lense focusing (for attractive force) in both planes. Such a lense can be included into the lattice to find the linear incoherent tune shift $\Delta\nu$ and the linear change of amplitude β-function. For one interaction place one gets, for example, for y-plane:

$$\cos 2\pi \left(\nu_y + \Delta\nu_y\right) = \cos 2\pi\nu_y - 2\pi\xi_y \left(\sin 2\pi\nu_y\right) \quad , \qquad (1.8)$$

$$\beta_y = \beta_{0y} \left(\sin 2\pi\nu_y\right) \Big/ \sin 2\pi \left(\nu_y + \Delta\nu_y\right) \quad , \qquad (1.9)$$

wherein appears the famous space charge parameter:[69-72]

$$\xi_y = \frac{\beta_{0y}\, Nr_0}{2\pi\gamma\sigma_y\left(\sigma_x + \sigma_y\right)} \quad . \qquad (1.10)$$

Analogous expression holds for ξ_x:

$$\xi_x = \frac{\beta_{ox}\, Nr_0}{2\pi\gamma\sigma_x\left(\sigma_x + \sigma_y\right)} \quad . \qquad (1.11)$$

In these expressions β_{0x}, β_{0y} mean the values of the corresponding unperturbed β-functions at the interaction point; ν_x, ν_y are the corresponding unperturbed tunes of the machine.

Unfortunately, these simple expressions hold only for a small portion of particles. As one can see from Figs. 1.1-1.6, the forces are strongly nonlinear for particles with $x/a \sim 1$ and $y/b \sim 1$. The nonlinear character of the beam-beam force brings up a whole set of nonlinear resonances with different m_x, m_y.

In addition to purely transverse resonances, there can appear (and play an important role) resonances due to coupling of transverse and longitudinal motion.[11] Such coupling arises for example for head-on collisions if at the interaction point the dispersion function or its derivative is not zero. Hence, horizontal synchrobetatron resonances appear in machines with the finite η_x^*. Similarly, both horizontal and vertical synchrobetatron resonances appear with finite spurious $\Delta\eta_x^*$ and η_y^* due to different lattice imperfections in all storage rings. Another example is crossing of the bunches at an angle either in horizontal or in vertical planes. In these cases the kick depends on both transverse displacement and longitudinal position of the particle in the bunch, providing a coupling between transverse and longitudinal motion. Still another synchrobetatron coupling effect caused by the beam-beam interaction occurs when the bunch length is not small compared with the beta-function value β_0 at the interaction point. In this case, the magnitude of transverse kick again depends on the longitudinal coordinate of the particle (due to the difference in particle distribution along the bunch), thus providing a coupling mechanism. Fig. 1.7 illustrates simulated and identified resonance lines due to the beam-beam interaction in the storage ring DORIS[10] for several few first numbers m_x, m_y. Of course, there must be infinitely more resonance lines, but the influence of a

resonance of higher order on the particle motion is small if its amplitude is not too big.

1.3 Two-Beams Coherent Dynamics

So far I have considered single particle motion taking the interaction with oncoming beam into account. Now, let us consider coherent effects in bunch motion which are brought about by the beam-beam interaction.

In linear approximation the beam-beam force induces dipole oscilations of bunches as a whole. The oscillations of different bunches are coupled to each other and can be described by their normal modes. Eigenfrequency of each mode should be chosen outside the stopband of all resonances. Figs. 1.8 and 1.9, taken from the work[5] present the stability regions for dipole oscillations of bunches for the cases of collisions of one-by-one and of three-by-three bunches correspondingly. Coherent space charge parameter is twice as big as the incoherent one since the beam-beam force seen by a center of a bunch displaced by y is the same as that for a single particle displaced by 2y in the incoherent motion.

The nonlinear terms in the beam-beam force can also cause higher multipole coherent oscillations. The analysis of these oscillations is much more complicated and involves difficult and cumbersome calculations.[12-14] Fig. 1.10 taken from the work[14] illustrates the widths of a few first resonances of coherent oscillations excited by the beam-beam interaction in the system with charge compensation.

1.4 Beam Blow-Up (Flipping)

For the conclusion of this long introduction it is useful to describe briefly what happens with the beams when they are collided. Normally, during storing process of both beams they are separated from each other at interaction points by means of special electrostatic fields (all other places of the machine circumference bunches pass at different time and do not disturb each other). When enough current is stored in each beam the separation field is switched out and particles start to interact producing the desirable (as well as the undesirable) effects.

The behavior of bunches now completely depends on the value of a current stored in both of them.

1.4.1 Weak-Beam — Strong-Beam Incoherent Instability

Suppose first, that the number of particles in bunch "1" (weak beam) is much less than that in the opposite bunch "2" (strong beam). In this case there exists a critical value of the current and correspondingly a critical value of the space charge parameter ξ_y of the strong beam. Below it there are hardly any visible beam-beam effects, but as soon as the threshold is reached the vertical size of the weak beam suddenly increases significantly (beam blow-up or flip). At the same time the horizontal size of the beam does not change significantly. The strong beam shows very small change, if any at all. Typical value of the crucial space charge parameter ξ_y is around 0.03 - 0.05. The space charge parameter of the weak beam being small because of its current, becomes still less due to increase in size. Fig. 1.11 illustrates beam blow-up in the experiment at SPEAR.[15]

Along with the change in the bunch size, the particle distribution also experiences significant change. The distribution deviates from simple Gaussian shape; the tails become much more populated.

Fig. 1.12 presents the results of vertical bunch profile measurements[16] on SPEAR for electrons and positrons before and after the separation was switched out.

The question of the rise time of the weak-beam—strong-beam instability is a difficult and still not resolved one. The attempts to measure it at SPEAR showed a value much smaller than the damping time. This fact was confirmed also on PETRA.

Although the weak-strong mode of operation is hardly used by any storage ring routinely, the study of the weak-beam—strong-beam instability is important. First of all this case is more simple to simulate on a computer since the strong beam can be considered as a source of an external constant force. This can give (and indeed does give) information on important factors to be included in considerations for the more complicated strong-strong case. To some extent the weak-strong case is also simplier from the theoretical point of view and still sheds some light on the whole problem.

1.4.2 Strong-Beam—Strong-Beam Incoherent Instability

The most usual mode of operation of a storage ring is one of maintaining the currents in both beams as equal as is practically possible. The main reason for this is of course the desire to achieve the maximum luminosity of the storage ring. Were the current of one beam less than that in another, the weaker beam would flip at much lower current magnitude, reducing the luminosity.

The strong-beam—strong-beam instability exhibits many common characteristics with the weak-strong case. One observes beam blow-up (usually bigger for the beam with slightly smaller current in it and smaller for the stronger beam), redistribution of particles in the bunch and increase of the population of its tails. The deviation from the Gaussian distribution is still more pronounced (See Fig. 1.13 for example. The illustration is taken from the work[4]). The change in particle distributions makes it extremely difficult to simulate strong-strong case in a computer study, since forces depending on the distribution should be recalculated for each interaction separately.

On the other hand there is no clear answer to the question of the existance of a threshold. It seems that in some cases such a threshold exists;[4] in other cases the beam blows up starting from very small values of the current.[17-19] The same holds for the tune dependence. In some cases there is marked dependence of the beam blow-up limits on the values of the tunes.[19,20] For the high beam intensity only a small island of stability can be found on the tune diagram. As an example, in Fig. 1.14 taken from the work[19] are shown the regions of stability for the ACO and DCI storage rings. At the same time, in some cases strong dependence on tune is not observed.[17] An interesting situation is with the storage ring SPEAR. In the old version of the machine (SPEAR 1) such dependence has been observed.[4] The beam-beam limit was raised by a factor of five by decreasing the vertical tune. Further decrease was impossible due to the existence of strong two-beam resonance $\nu_x - 2\nu_y = 5$ (forbidden for the two-fold symmetry of the machine with one beam). This effect disappeared in the modified machine (SPEAR 2).[4]

The fate of the blown-up beam strongly depends on the beam current and the energy. At the maximum currents and energies for a given storage ring the lifetime of the beam is reduced drastically and beam is usually lost in very short time. At smaller currents or energies the lifetime of the blown-up beam seems to be unaffected and equal to the lifetime of the unblown beam.[21] This can be used to restore normal conditions, by using strong dependence of the blow-up on the machine tunes.

It is worthwhile to mention here that near, but below, blow-up limit the beams are highly sensitive to all kinds of perturbations. Even a small change of conditions usually causes the beam blow-up.

The dependence of the effect on the number of bunches is also still not understood completely. The intensity of the beam-beam interaction increases with the increase of the number of bunches. In principle this should lead to the decrease of the luminosity at the given interaction place and to the decrease of the beam-beam limit. There are observations showing indeed such dependence;[21,22] but there are also others,[26] which can be interpreted as exhibiting maximum luminosity independent of the number of bunches.

1.4.3 Flip-Flop Effect

A remarkable controlled beam blow-up is discovered on SPEAR.[22] At certain conditions, by changing the difference of the phase of two accelerating cavities, it is possible to blow-up one (flip) or another (flop) of two beams. The flip-flop effect is apparent only near the beam-beam limit at a given energy. There is also pronounced influence on the effect of the magnitude of the horizontal dispersion function at

the interaction point. Other parameters of the ring (chromaticities, sextupole strengths, bunch length, tunes and coupling) seem to be important or not depending on the question of whether or not they influence the separation of the bunches or the horizontal dispersion at the interaction point of the machine.

The complete understanding of the flip-flop effect is not yet achieved. Nevertheless the effect is successfully employed to balance the heights of the opposite bunches at the maximum current, hence maximizing the luminosity of the ring.

Preliminary observations[23] show the existance of the flip-flop effect also in PETRA.

2. EXPERIMENTAL OBSERVATIONS

The comprehensive review of the experimental results obtained with different storage rings is not an easy job. The difficulty arises not only because of wide spectra of different types, and quite different parameters of the storage rings (energy, space charge parameters, currents, number of bunches and so on) but mainly because of completely different conditions of the measurements and the different ways of interpreting results.

Even for a given storage ring the results strongly depend on the tunes, energy, quality of closed orbits correction, chromaticity, transverse offsets of the bunches at the interaction point, assymetry of the ring (differences in phase advance between the interaction points), aspect ratio of the bunch and so on, almost ad infinitum.

To make the task easier, I will first of all concentrate on electron storage rings, for which data are much more abundant. For proton storage rings only the illustrative example of the CERN Interacting Storage Ring (ISR) will be given.

Before discussing recent experimental results observed on different storage rings, it is useful to look first at the conditions in which they are obtained and the assumptions under which they are interpreted.

2.1 Main Relationship and Assumptions

First of all let us discuss relevant storage ring parameters as well as experimental conditions under which they are usually measured. I will list the main parameters and relationships between them, although the latter are all well known.

2.1.1 Luminosity

Luminosity of the storage ring for the head-on collision of two identical beams is usually assumed to be

$$\mathscr{L} = \frac{i^2}{4\pi e^2 f B \sigma_x \sigma_y} \tag{2.1}$$

where i is the current in either of two beams, B is the number of bunches in each of the beams, f is the revolution frequency of the particle with charge e, σ_x and σ_y are horizontal and vertical dimensions of the bunch (rms widths if the distribution is Gaussian) at the interaction point. Useful physics experiments can be done with the storage ring if the luminosity is on the order of 10^{30} cm^{-2} sec^{-1} for the 5 GeV energy range. For higher energy this value should rise as E^2.

2.1.2 Space Charge Parameters

Space charge parameters under the same conditions are given by the following formulae (compare 1.10 and 1.11).

a) for the vertical motion:

$$\xi_y = \frac{ei\beta_y}{2\pi f BE\sigma_y(\sigma_x + \sigma_y)} \quad , \tag{2.2}$$

b) for the horizontal motion:

$$\xi_x = \frac{ei\beta_y}{2\pi f BE\sigma_x(\sigma_x + \sigma_y)} \quad . \tag{2.3}$$

In these formulae β_x and β_y are values of horizontal and vertical β-functions at the interaction point; E is particle energy. Both the luminosity $\mathscr{L}$ and the space charge parameters ξ_y and ξ_x depend on the bunch size which is very difficult to measure directly. But it is clear

that both values are sensitive to the charge distribution in the core of the beam rather than to the tails of it. At the same time, it is known[4] that tails are affected by the beam-beam interaction much more strongly than the core.

2.1.3. Lifetime

The beam lifetime T for a single Gaussian bunch is given by[24]

$$T = \frac{\tau e^{\zeta/2}}{\zeta} \quad , \tag{2.4}$$

where τ is the vertical damping time

$$\frac{1}{\tau} = \frac{C_\gamma \oint E^3}{2\rho} \quad , \tag{2.5}$$

$C_\gamma = 8.85 \times 10^{-5}$ m/GeV^3, ρ = bending radius in m, and E the energy in GeV.

$$\zeta = \frac{\Sigma^2}{\sigma^2} \quad . \tag{2.6}$$

Here Σ is an effective aperture of the machine. The beam lifetime is sensitive to the distribution of the particles in the tails where the beam-beam interaction changes distributions significantly. That makes the maximum luninosity strongly dependent upon the value of the maximum beam current which in turn happens to be a fast function of the particle energy.

2.1.4 Parameters Known, Measured and Assumed

Among the machine parameters entering into expressions (2.1-2.6), the energy E, the number of bunches B, and the revolution frequency f are known with great accuracy. The luminosity $\mathscr{L}$ and the beam current i can be measured directly.

On the other hand, several other parameters (such as β_x, β_y) are difficult to measure. Although one can expect that β_x, β_y should be modified by the beam-beam force, these functions are changed only in the second order of the perturbation theory and therefore usually are assumed to be equal to their theoretical value at the zero current. The same holds for the horizontal beam emittance ε_x and consequently for the horizontal beam size $\sigma_x = \sqrt{\varepsilon_x \beta_x}$.

2.1.5 Experimental Conditions and Assumptions

Experimental data on the beam-beam effect are obtained on different machines virtually in quite different conditions.

a) The investigation of the beam-beam limitations. Measurements of this kind are done during special machine physics runs. The main goal of these measurements is to achieve the maximum possible luminosity for given parameters by increasing the currents to the point where the lifetime of the beam starts to decrease sharply. To maximize the luminosity of the ring both currents are usually maintained pretty much the same. For the SPEAR measurements[25]

$$\frac{2(i_+ - i_-)}{(i_+ + i_-)} \lesssim 10\ \%$$

One tries to do the same with the vertical size of the beam. At least at SPEAR this condition was met by means of adjustment of the phase between the rf cavities positioned symmetrically around the interaction point.[22]

Experimental data obtained in this situation should be more sensitive to the particle distribution at large amplitudes (to the tails of distribution) rather than to the distribution in the core of the beam.

b) The investigation of the storage ring performance. Measurements of this kind are usually done during high energy physics runs in a parasitic mode. Maximum luminosity is achieved in this case under a restrained condition of the beam lifetime being affected by beam-beam phenomena or by demand to have reasonable background in experimental devices. These measurements should be more sensitive to the distribution in the core of the beam.

c) It is important also to distinguish the regions of parameters below and above the blow-up limit. The boundary between these two conditions is not always sharp and pronounced. Since the functional behavior of relevant parameters is quite different in these two regions, one should be specific when talking about their values and dependencies on energy, current, bunch number and the like.

In all of the storage rings the longitudinal size of the bunch σ_ℓ is much less than β_y. If this condition were not fulfilled, different particles along the bunch would experience different focusing and the results could be distorted by this effect. As we shall see later, it is assumed usually that the distribution of the particles is Gaussian, at least in the core. One needs this assumption to be able to calculate the space charge parameters from the measured luminosity and current. In some aspects there is also a difference between the strong-beam—strong-beam and the strong-beam—weak-beam interactions.

2.2 Experimental Results

An experimental fact observed on all the machines is that the horizontal size of the bunch is not influenced by the beam-beam interaction[4,26] with the accuracy $\lesssim 10\%$.

2.2.1 Procedure

It is instructive first to see how one can derive the relevant parameters from the measured ones.

First of all, assuming σ_x to be equal to $\sqrt{\varepsilon_x \beta_x}$, one can find beam aspect ratio σ_y/σ_x from the measured luminosity (2.1):

$$\frac{\sigma_y}{\sigma_x} = \frac{i^2}{4\pi e^2 f B \sigma_x \mathscr{L}} \tag{2.7}$$

Formula (2.3) then allows us to find the horizontal space charge parameter

$$\xi_x = \frac{ei\beta_x}{2\pi f BE \sigma_x^2 \left(1+\sigma_y/\sigma_x\right)} \tag{2.8}$$

After eliminating σ_y from (2.1) and (2.2) one gets:

$$\xi_y = \frac{2 e^3 \mathscr{L} \beta_y}{Ei \left(1+\sigma_y/\sigma_x\right)} \tag{2.9}$$

Let us review now the recent experimental results obtained on different storage rings.

2.2.2 SPEAR. Dependence on Energy

Recently a set of new measurements of the maximum luminosity and the beam current versus machine energy was undertaken by H. Wiedemann.[27] The range of energy variation was from 0.6 to 3.7 GeV and is much wider than in all previous experiments. The data are taken during the special runs of the SPEAR dedicated to machine physics. Much work is done to adjust all the machine parameters to achieve maximum luminosity. Special attention was paid to balance the vertical sizes of electron and positron bunches to avoid the loss of the luminosity due to the blow-up effect.

The fit by a power law to recent data seems to give quite different slopes, especially for the vertical space charge parameter, than ones in the previous measurements.[4] The difference may be attributed to the fact that the energy range in the work[4] was much narrower (from approximately 1.2 to 2.5 GeV). Table 1 summarizes the results of fitting to these measured and calculated data.

2.2.3 SPEAR. Dependence on the Beam Current

Table 2 summarizes the data picked up from SPEAR logbooks by M. Cornacchia.[28] The data were mostly taken during regular physics runs of the machine. The fits to the data taken at high energy physics run are recalculated. Instead of fitting data by the least square method the maximum luminosity was fitted.

2.2.4 ADONE

Table 3 summarizes the dependencies of the maximum luminosity and the beam current versus energy which were taken from the report by S. Tazzari.[21] The space charge parameters of this machine were kept approximately equal to each other. The fit for the space charge parameters is derived from the calculated values plotted in the work.[21] The number of bunches in ADONE can be and were changed. The data taken with one and three bunches do not contradict the assumption

$$\xi_y \sim \frac{1}{\sqrt{B}} \quad .$$

2.2.5 PETRA

The data from the measured specific luminosity $\mathscr{L}B/i^2$ during high energy physics experiments were fitted with the help of the blow-up

function σ_y assumed[17] to behave according to the following:

$$\sigma_y^2 = \sigma_0^2 + \left(\frac{ai}{\sigma_y}\right)^2 \quad . \tag{2.10}$$

Here σ_0 is the value of σ_y at zero current i and a is a parameter. From the data taken at different energies, a is found to be:

$$a = \frac{\text{const}}{E^4} \quad . \tag{2.11}$$

The values of aspect ratio of the beam emittances are estimated to be of the order of several percent at all energies.

2.2.6 PEP

Due to sixfold symmetry of the machine, the operation of PEP is performed in one-by-one or three-by-three bunch modes. The beam-beam data obtained in these modes differ from each other. The reason for this difference is not yet understood.[29] Figures 2.1 - 2.3 present the results[30] of measurements of the luminosity, the specific luminosity $\mathscr{L}/BI_B^2$ and the vertical tune shift $\Delta\nu$ for different bunch currents. The data are taken with the particle energy 14.5 GeV. It is clearly seen that the initial slope of $\mathscr{L}(I_B)$ for 1×1 mode agrees with the I_B^2 law (constant cross section of a bunch). The function saturates at higher current values indicating the cross section increase (blow-up). At the same time the luminosity curve for 3×3 mode does not seem to follow I_B^2 law even for very small current. The same, but more clearly, can be seen from the specific luminosity data. The 3×3 data show beam blow-up starting from the lowest available current data.

Unfortunately, there are not enough data to fulfill the analysis similar to one of PETRA. More data for different energies is needed for the comparison between two storage rings.

2.2.7 CESR

Luminosity measurements and observations of the related beam-beam effect is done[73] on this storage ring at the energy 5.5 GeV (the designed energy of the ring is 8 GeV). The maximum luminosity of $3\times10^{30}\ cm^{-2}\ sec^{-1}$ has been achieved which corresponds to a maximum vertical tune shift of 0.035. Luminosity curves versus current show i^2 dependence up to $i \lesssim 4$ ma for different lattice configurations. Above this value one or both beams flip and the saturation is seen clearly. It is found that small changes in tune can lead to large changes in specific luminosity and/or lifetime of the beam.

2.2.8 Low Energy Machines

The summary of experimental observations on several other machines can be found in Table 4, which is taken from the work.[31] Representative samples of data for SPEAR taken from work[27] and for VEPP-4 taken from work[74] are added. The first four columns give the maximum energy, the vertical tune ν_y, the vertical β-function at interaction point, β_y, and the number of bunches per beam. The next four columns deal with scaling laws for maximum current, luminosity, beam cross-section and the beam strength parameter as a function of energy. The last column gives the maximum value of the beam strength parameter ξ_{max} achieved.

2.2.9 Intersecting Storage Rings (ISR)

To give the reader the feeling of the order of magnitude of relevant parameters for proton bunched beams, I include here the results of the beam-beam study,[32] undertaken on the Intersecting Storage Ring at CERN. While for the electron storage ring the beam-beam shift tune is of the order of 0.03 - 0.05, the maximum achieved value for the same parameter

for the protron storage ring is 3×10^{-3}. This value is obtained for well adjusted vertical position of two beams at the interaction point. When beams were off-centered by approximately one standard deviation, dramatic blow-up was observed. The rate of the vertical blow-up increases substantially, also by the noise in the bunching RF system.

For continuous beams the beam-beam limit was observed[33] to be in the range 0.01 - 0.02. The difference between this result and the results for bunched collisions is believed to be attributed to the fact that for continuous beams the motion is essentially one-dimensional (since the vertical tune shift is much larger than the horizontal one, while there are no synchrotron oscillations). For one-dimensional motion one can expect the presence of a stable region below the "stochastic limit".

3. THEORETICAL MODELS AND TECHNIQUES

At the present time there is no satisfactory theory for the beam-beam phenomena. The complexity of the physical object being, essentially, extremely hot plasma very far from the equilibrium makes the analysis very difficult. The situation is aggravated also by the highly nonlinear character of the beam force, the presence of other nonlinearities in the equation of motion, the influence of noise of different origins, and by nonuniformity in space (aperture of the machine) and time (damping).

There are many approaches to the problem and many theoretical and computational techniques being used in the attempt to attack the problem. Many of these give qualitative explanation to some observed facts, but it is hardly surprising that all of them are unable to give comprehensive description of the phenomena as a whole, nor able to give ways and means to calculate the relevant parameters. As we shall see from the review of these different approaches even proper understanding of which factors are important and which are not is still to be achieved. I think we are still far from formulating proper parametrization of the problem: different theories give different sets of important parameters!

Hardly in better shape is computational technique. Until now all computer simulations have been restricted to particle tracking. In most cases the results of tracking are difficult to interpret in terms of real machine parameters. In better cases, these results seem to be satisfactory to their authors and can be applied only to one particular machine for which they are designed. There is also one practically important restriction of the tracking method. If as I believe to be true, the nonlinear elements (sextupoles) of the machine are important

for correct description of the beam-beam phenomena, then the capacity of modern computers is not enough to do the job, at least for the future big machines since computing time becomes forbidding. Still more this is true for proton machines. While for electron storage rings, it is believed that only several damping times are essential to get to the stationary state ($\sim 10^3 - 10^4$ collisions), for the proton ring such time should be the lifetime of the beam ($\sim 10^{10} - 10^{11}$ collisions) which is far beyond the ability of any computer.

In subsequent sections I try to describe very superficially some different theoretical models. The aim of this description is to inform the reader of the main underlying ideas and obtained results. It is not intended here to go into details of sometimes very complicated mathematics.

I have restricted myself to the beam-beam interactions in a storage ring. There is a related subject, that of the beam-beam interaction in a linear collider. Some interesting theoretical and computational work[62-66] has been done in this area. This work helps to look into the beam-beam phenomena, studying it in a self-consistent manner; but since it lies out of the topic of our workshop (long-time prediction), and mainly because no experimental observations have been done yet, I do not include the subject in the present review.

3.1 Single Resonance Models

I follow here the work[5] where one can find more details as well as some references to other papers on this subject.

Two main assumptions lie in the foundation of the model:

a) There is only one set of integers, q,p,n, satisfying the condition $q\nu_x + p\nu_y \simeq n$, which dominates the motion of a single particle

interacting with a fixed opposite bunch. In principle there are many other sets of numbers, p,q satisfying this condition. The rational to ignore them is that the influence (width) of corresponding resonance drops faster with the increase of the particle amplitude the more quickly the numbers p and q increase.

b) All the fast oscillating terms in the equation of motion can be ignored (smooth approximation). Formally that goal is achieved by substituting the Hamiltonian by its average over unperturbed phase trajectory. Such averaging changes the volume of the phase space, which can lead to some errors. Besides that, this approach does not take into account the existence of stochastic regions and possible Arnol'd diffusion.

Two such models will be discussed. In the first one all parameters are considered to be constant (static model). The second model allows slow (adiabatic) change of the parameters due to coupling to longitudinal motion (dynamic model).

3.1.1 Static Model

Consider transverse motion of a single particle in the presence of a fixed opposite bunch (weak-beam—strong beam case neglecting synchrotron oscillations).

The Hamiltonian of this problem is:

$$\mathcal{H} = \frac{1}{2}\left(px^2 + K_x(s)x^2\right) + \frac{1}{2}\left(py^2 + K_y(s)y^2\right) + U(x,y)\ \varepsilon(s) \quad , \quad (3.1)$$

where $K_x(s)$ and $K_y(s)$ are lattice horizontal and vertical focusing functions of the longitudinal coordinate s. Potential of the beam-beam interaction U(x,y) should be chosen in such a way as to give correct

"kicks" $\Delta x' = -\partial U/\partial x$ and $\Delta y' = \partial U/\partial y$ (see 1.4 and 1.5). Periodic function $\varepsilon(s)$ describes the longitudinal dependence of beam-beam force. For short bunch it can be approximated by the δ-function periodic in s. In the vicinity of the single resonance $q\nu_x + p\nu_y = n$ (assumption 1) the Hamiltonian has fast oscillating and slowly changing terms. The averaging procedure (assumption 2) throws the fast oscillating terms away. If the particle distribution in the strong bunch is Gaussian and its action can be described as a δ-function kick in time, the remaining Hamiltonian depends on five dimensionless parameters,

$$\xi_x, \quad \xi_y, \quad \nu_x, \quad \nu_y \text{ and } \frac{\sigma_y}{\sigma_x} \quad .$$

The tune shift $\Delta\nu$ and the width of resonance $\delta\nu$ as functions of particle amplitude can be calculated. For the one-dimensional case ($q = 0$) the result is:

$$\Delta\nu(\alpha) = \xi\, e^{-\alpha} \left[I_0(\alpha) + I_0'(\alpha)\right] \quad , \tag{3.2}$$

$$\delta\nu(\alpha) = 8\xi \sum_s \left| \frac{e^{-\alpha} \left[(1+2\alpha)\, I_{sp/2}(\alpha) + 2\alpha I_{sp/2}'(\alpha)\right]}{s^2p^2 - 1} \right| \tag{3.3}$$

where $\sqrt{2\alpha}$ is the normalized amplitude in units of the strong bunch vertical dispersion

$$\alpha = \frac{J\beta}{2\sigma^2} \tag{3.4}$$

and I_m is the modified Bessel function of the m^{th} order. Qualitative behavior of $\Delta\nu$ and $\delta\nu$ are shown in Fig. 3.1.

Due to fast decay of the resonance width with the amplitude according to the static model, the motion is stable in respect to beam-beam interaction in striking contradiction to experimental observations. This discrepancy seems to be overcome by dynamic models.

3.1.2 Dynamic Models: Trapping

The static model does not provide a mechanism for transporting particles from small to large amplitudes. Such mechanism seems to be necessary to provide for particle losses and lifetime decrease. There are several models[34-36] with time variable parameters, such as ν or ξ, which lead up to an instability. The change of the parameters may arise from different sources. It may be coupling to longitudinal motion, in which case the tune ν may be modulated by synchrotron frequency ν_s, or it may be some noise in the system causing the tune diffusion. The change of the tune makes the assumption 1 (single resonance) still less sound then for the static model.

In the work[36] it is assumed that the space charge force can be considered as a source of the tune diffusion via the tune dependence on amplitude. Diffusion through the single resonance leads to amplitude growth. Assuming the $\bar{\nu}_{res}$ to be constant, the author finds the following expression for the beam-beam limit:

$$\frac{\xi^2}{\gamma^{3/2}} = \text{const} \tag{3.5}$$

which gives the dependence of the maximum current and luminosity as functions of energy:

$$I_{max} \sim \gamma^{3.75} \tag{3.6}$$

$$\mathscr{L} \sim \gamma^{5.5} \tag{3.7}$$

(assuming $\sigma_x, \sigma_y \sim \gamma$).

The dependencies (3.5) and (3.7) seem to be too slow for reasonable agreement with experimental observations.

This model seems to have a support from the computational simulation of J. Tennyson,[37] where streams of particles are discovered along a certain resonance tube toward larger amplitude, where they are dropped out.

In the trapping model[34] the tune of the particle is adiabatically changed in time close to a single resonance value n/p. These changes cause the resonance islands (the separatrixes) to move. At a certain rate of the time change it is possible that an island will trap a particle bringing it from one phase trajectory to another. The islands movement is completely analogous to the autophasing in longitudinal motion in a synchrotron, where slow increase of the magnetic field causes the separatrix to move toward bigger mean energy. Synchrotron oscillations of the particle inside the separatrix then follow its movement exibiting the example of trapping. As we know, the speed of the magnetic field change should not exceed a certain limit, which is determined by the dependence of the revolution frequency on energy. At this value the size of the separatrix becomes zero. In the same manner the speed of the tune change in the trapping model should not exceed a certain limit, which in turn is determined by the amplitude dependence of the tune, at which the width of the island tends to zero.

To find the rate of particle transport toward larger amplitudes in the trapping model one needs an evaluation of the trapping probability. It is assumed that this probability is proportional to the volume of the island, being small for small amplitudes. It then reaches its maximum at a dimensionless amplitude of the order of magnitude 1-3 (depending on the order of the particular resonance) and then drops toward larger amplitude again (the decrease is due to both the

decrease in resonance width and the distance to resonance). The net effect then is the difference of the number of particles brought from the small to large amplitude (proportional to particle density inside the bunch) and the number of particles brought back from larger to smaller amplitude (proportional to particle density in the tails of distribution).

3.1.3 Method of Lie Transformation

The application of the transfer map method[38] to analysis of the beam-beam interaction will be discussed here very briefly, since the main contributor to this method, A. Dragt, will present the topic himself.

General nonlinear transfer map m is an operator transforming phase coordinates

$$z = \left(q_1, q_2 \cdots q_n, p_1, \cdots p_n\right) \tag{3.8}$$

from one Poincare section to another

$$z_2 = m z_1 \tag{3.9}$$

The map m depends on coordinate z_1. Action of each element of the lattice (linear or nonlinear) on coordinates z_1 at the entrance can be considered as a map transfering them into coordinates z_2 at the exit. Hence any m can be constructed as a product of m_i for each element.

For any function in phase space f(z), a corresponding Lie operator F can be defined. It is acting on any other function g(z) according to the following rule:

$$Fg = \left[f,g\right] \tag{3.10}$$

Here [f,g] denote Poisson bracket for functions f and g. Hence the Lie operator is a linear differential operator in the phase space.

For example, the Lie operator P_i associated with the particle momentum p_i is

$$P_i = -\frac{\partial}{\partial q_i} \quad . \tag{3.11}$$

This is very similar to the quantum mechanical operator of momentum, the fact which has very interesting consequences in the new approach to classical mechanics.[39]

It is possible to construct from the Lie operator F a Lie series as a power series of F. Of special interest is the exponential series, called Lie transformation:

$$\exp(F) = \sum_{n=0}^{\infty} \frac{F^h}{h!} \quad . \tag{3.12}$$

It was shown,[40] that any m_i can be presented in the form $\exp(F_i)$. For example, consider any linear piece of ring with phase advance ψ_x and ψ_y of transverse oscillations. Then corresponding Lie transformation e^F is constructed from the operator F associated wtih the quadratic polynomial

$$f_{(2)} = -\frac{\psi_x}{2}\left(x^2 + p_x^2\right) - \frac{\psi_y}{2}\left(y^2 + p_y^2\right) \quad . \tag{3.13}$$

The Lie operator for a sextupole magnet is associated with the cubic polynomial

$$f_{(3)} = Q_x x^3 - Q_y xy^2 \tag{3.14}$$

where Q_x and Q_y are values proportional to the strength of the sextupole magnet, and so on.

Similarly can be constructed the Lie operator for the action of the strong bunch on a particle motion. The corresponding Lie operator is associated with the potential function of the electromagnetic interaction.

The remarkable feature of the Lie transformation method is the fact that the canonical map can be presented as a product of corresponding Lie transformations depending on initial coordinates only, thus generalizing the matrix method of analysis to nonlinear mechines.

This method was used recently to study a one-dimensional model of the weak-beam—strong-beam interaction. The strong bunch is assumed to have round cross section. The Hamiltonian of the motion can be found explicitly for two cases: far from any resonance as well as near a single resonance of order p. The motion is found stable for any tune shift parameter of physical significance. This is hardly surprising since we have already seen the same result for the same model, studied by a different method (see section 3.1.1). Still I believe that the beauty and power of this method will give many more interesting results and not only in the study of the beam-beam interaction, but also in investigations of many other aspects of nonlinear behavior of storage rings.

3.2 Many Resonances Models: Stochastic Limit

The assumption which is made in simple resonance models does not appear to be very realistic. A picture of the simultaneous action of many resonances together seems to be closer to reality. As far as the strength of the beam-beam interaction is small enough, the separation between the different resonances (at least for low order resonances) is greater than their widths. In this case the Kolmogorov-Arnol'd-Moser theorem is valid and the motion of almost all particles with different initial conditions is stable, deterministic and reversible in time. The trajectories of such particles are only slightly perturbed by the

presence of resonance. There are exponentially thin layers in the phase space (near the separatrixes associated with resonances) where particles which happen to be there due to initial conditions behave erratically. In one-dimensional systems the KAM surfaces are closed and provide stability even for a particle inside such a layer. In multidimensional systems the layers associated with different resonances can intersect each other making it possible for the particle in the layer to drift from one resonance to another and eventually away to the machine aperture (so-called Arnol'd diffusion). This would not practically reduce the bunch lifetime unless there is no external noise in the equations of motion which can occasionally bring more and more particles inside the stochastic layer.

The situation changes drastically with increase of the strength parameter. At a certain value of this parameter the widths of the next resonances become big enough to touch each other. The KAM surface breaks down and the motion becomes stochastic for a substantial portion of the phase space (initial conditions). This resonance overlapping situation is believed to create the beam-beam limit and is a content of the Chirikov criterion for stability.

In the following I describe very briefly (just for completeness of the review) the most important ideas developed along this line. The subject links the problem of beam-beam interaction to the more general problem of long-time behavior of the nonintegrable Hamiltonian systems and exhibit some basic concepts of nonlinear Hamiltonian Dynamics: resonance, closed orbits, stochasticity and Arnol'd diffusion. More comprehensive description and more details will be presented in the

next few talks and can be found in literature (see for example[45-47] and references therein).

3.2.1 Estimate of the Beam-Beam Limit According to Chirikov Criterion

Let us evaluate the beam-beam limit according to Chirikov criterion.[48] I follow here the derivation of the work.[49] Practically the same treatment is used by Bountis.[46] One finds an interesting approach[50] expressing Chirikov criterion in terms of a turbulence limit of a flow in the phase space.

Consider one-dimensional motion of a particle in the presence of the second bunch. The Hamiltonian of the motion in action-angle variables is

$$H = \nu J + \sum_{m,k=-\infty}^{\infty} \varepsilon_{km}(J)\, e^{i(m\phi - k\theta)} \tag{3.15}$$

Term $\varepsilon_{00}(J)$ determines the dependence ot the oscillation frequency on amplitude:

$$\alpha = \frac{d\omega}{dJ} = \frac{d^2\varepsilon_{00}}{dJ^2} \tag{3.16}$$

For δ-function like perturbation in θ, ε_{km} does not depend on k. If ε_m is small enough each of the other terms in (3.15) produce a resonance at the frequency

$$\omega_{km} = \frac{k}{m} = \nu + \alpha J_{km} \tag{3.17}$$

The last equation in (3.17) determines the resonant amplitude J_{km}.

In phase space a resonance is surrounded by a separatrix the width of which is

$$\delta J_{km} = 4\sqrt{2\varepsilon_m (J_{km})/\alpha} \quad . \tag{3.18}$$

The same value in terms of frequency is:

$$\delta\omega_{km} = \alpha\Delta J_{km} = 4\sqrt{2\alpha\varepsilon_m(J_{km})} \quad . \tag{3.19}$$

The resonance separation around the resonance of the order m is $\Delta\omega_{km} \simeq 1/m$. Now Chirikov criterion can be formulated quantitatively if one finds the sum of the ratio of the widths to the separtions in a unit frequency interval. If one introduces the notation

$$\frac{1}{\lambda} = \sum_m m\sqrt{2\alpha\varepsilon_m(J_{km})} \quad . \tag{3.20}$$

then Chirikov stability criterion becomes

$$\lambda > 4 \tag{3.21}$$

The numerical investigation of the validity of this criterion on the model called the standard mapping[51] shows that (3.21) overestimates stability (actual loss of stability appears for a smaller value of ε).

The same seems to be true for the beam-beam stability limit at least in the simple one-dimensional model with the round Gaussian strong bunch. Expression (3.21) gives in this case, for the space charge parameter:

$$\xi < 1/8 \quad , \tag{3.22}$$

which is clearly 3 - 4 times better than the experimental observations.

It is common thinking that the limit will look more realistic for bunched beams if one takes into account the existance of additional synchrotron resonances arising due to coupling of the transverse motion to the longitudinal one. The overlap of synchrobetatron resonances has been studied by Israilev[52] where it is shown that indeed the beam-beam limit can be reached at $\xi \approx 0.04$. For unbunched proton beams the more

severe limit is believed to be connected with Arnol'd diffusion—in the absence of damping the needed lifetime can be achieved only below the stochastic limit when resonance overlapping has not developed to full scale.

3.2.2 Study of Nonlinear Equations of Motion

It is worthwhile to mention here a completely different approach to the beam-beam problem in which the stability limit is searched from the investigation of the nonlinear Hill's equation[53,54] or corresponding finite difference equations.[55]

Again the one-dimensional problem is investigated. Consider two first-difference mappings

$$x_{t+1} = y_t \quad , \tag{3.23}$$

$$y_{t+1} = -x_t + 2y_t \cos 2\pi\nu + \xi F(y_t) \frac{\sin 2\pi\nu}{\nu} \tag{3.24}$$

describing the vertical motion in the presence of the δ-function beam-beam force $\xi F(y)$, ξ being the strength parameter. For the piecewise linear beam-beam force

$$F(y) = \begin{cases} y & \text{for } |y| < \frac{\sqrt{\pi}}{2} \\ \frac{\sqrt{\pi}}{2} & \text{for } y > \frac{\sqrt{\pi}}{2} \\ -\frac{\sqrt{\pi}}{2} & \text{for } y < \frac{\sqrt{\pi}}{2} \end{cases} \tag{3.25}$$

It appeared possible to construct an invariant curve y(x) in the phase plane, i.e., the curve invariant in respect to the nonlinear map under consideration. It contains a stable region of the motion for all times.

For each given value of ν only one such curve is found to exist. The stability limit is determined from the following expression:

$$\Delta\nu = \frac{\xi}{4\pi\nu} = \frac{\cos 2\pi\nu(1+\cos 2\pi\nu)}{\pi(1+2\cos 2\pi\nu)(-\sin 2\pi\nu)} \quad . \tag{3.26}$$

For the ISABELLE storage ring this gives $\Delta\nu \approx 0.03$. This value seems again to be too optimistic.

3.3 Diffusion Model

We have seen above the attempts to describe the beam-beam limit as a combined effect of a single resonance and diffusionlike change of its parameters. In the case when there are many rather strong resonances inside the tune change region of the particle, the motion of the particle can become stochastic even in the absence of special noise sources. That circumstance makes it plausible to try to consider the beam-beam interaction in the limit where there is no correlation between the results of different collisions and between the phases of a particle at different interaction points.[41-44] Such considerations do not pretend to constitute a rigorous theory but rather a phenomenological model which helps to make parametrization of the experimental data in a suitable way and to derive some scaling laws by means of a few fitting parameters. The behavior of these fitting parameters is not described by a theory and should be taken from the comparison with an experiment.

It is useful first to go through main assumptions under which such models are developed as well as those which will be used in the following considerations.

First of all we shall consider a one-dimensional model of the beam-beam interaction. Although the phenomenon is essentially multi-dimensional, the justification of this model at least in the first approximation comes from the experimental observations that the vertical size of the bunch is most strongly affected by the interaction while the horizontal size of the bunch seems to be affected very little if any.

One may argue about the loss of some particular multidimensional features such as the Arnol'd diffusion, sideband resonances, and the like. All of these effects may be considered to be included in assumed particle stochastic behavior.

Secondly, we assume that at least some number of particles behave stochastically. The reason for such a behavior can be nonlinearities in the machine lattice, nonlinearity of the electromagnetic beam-beam force, combined action of many close-lying resonances, presence of a stochastic layer in the phase space of particle motion, etc. Note that I do not include in this list the change of particle amplitude due to radiation quantum fluctuations making thus the consideration equally applicable to proton storage rings.

We shall use in forthcoming considerations an assumption that both beams are identical. This assumption is not mandatory for the derivations but is justified by experimental conditions and makes all formulae more straightforward.

Also everywhere where it is appropriate, I will simplify the calculations using Gaussian distribution, linear force, etc. Although more exact calculations can be fulfilled sometimes they do not seem to be necessary due to oversimplifying assumptions made above already.

3.3.1 Beam Blow-Up

At each interaction the vertical coordinate y and the angle in vertical plane y' are changed as follows:

$$\Delta y = 0 \tag{3.27}$$

$$\Delta y' = 2\pi\xi_y \frac{\sigma_0}{\beta_y} K_b\phi_b(u) \tag{3.28}$$

where $b = (\sigma_y/\sigma_x) / \sqrt{1-(\sigma_y/\sigma_x)^2}$, $u = y/\sigma_0$ and $K_b\phi_b$ is a function describing the electromagnetic force of the opposite bunch. For Gaussian distribution[15]

$$K_b = \sqrt{\frac{\sqrt{1+b^2}+b}{\sqrt{1+b^2}-b}} \tag{3.29}$$

$$\phi_b(u) = u \int_0^1 \frac{dw}{\sqrt{u+b^2}} \ell^{-wu^2} \tag{3.30}$$

According to the main assumption a certain part of the motion due to the interaction (3.28) can be described as stochastic and the beam-beam interaction can be considered as an additional source of diffusion (in addition to all other sources which do not depend on the beam-beam force).

We know that at least the linear part of the force cannot cause the stochasticity. It can be considered as an additional focusing force and hence should be included in the regular part of particle motion. Probably the same is true also for some nonlinear parts of the force.

That is why for the purpose of calculating beam blow-up as a consequence of a diffusion-like process we should consider not all the force $\phi_b(u)$, but only some nonlinear part of it $\tilde{\phi}_b(u)$. The way to get $\tilde{\phi}_b$ out

of ϕ_b is not clear and should be considered here only as a way to introduce in the theory a phenomenological fitting parameter. It can be done in different manners:

$$\tilde{\phi}_b(u) = \begin{cases} \phi_b(u) - (1-h)\,\phi_b\left(\frac{u}{1-h}\right) , & \text{S. Kheifets}^{15} \\ h\phi_b'(u) , & \text{A. Ruggiero}^{44} \end{cases} \tag{3.31}$$

One can find still other possibilities. For a small value of h, both procedures give essentially the same result.

It is reasonable to assume that for particles which behave erratically there is a complete mixing of phases within the bunch and in the long run each particle can be expected to acquire any value of coordinate y. In this case the beam blow-up can be found by averaging the value $(\Delta y')^2$ over the distribution function

$$\sigma_y^2 = \sigma_0^2\left(1 + \eta \left\langle K_b^2 \tilde{\phi}_b^2 \right\rangle\right) , \tag{3.32}$$

where the brackets $\langle\ \rangle$ mean averaging over the distribution function. In expression (3.32)

$$\eta = 2B \oint \tau\left(2\pi\xi_y\right)^2 , \tag{3.33}$$

where τ is the vertical damping time (2.5)

For Gaussian distribution

$$\left\langle K_b^2 \tilde{\phi}_b^2 \right\rangle = \frac{K_b^2}{\sqrt{\pi}\,\frac{\sigma_y}{\sigma_0}} \int_{-\infty}^{\infty} \tilde{\phi}_b^2(u)\, e^{-\sigma_0^2 u^2/\sigma_y^2}\, du \tag{3.34}$$

Instead of doing actual calculations we substitute in the following

$$\tilde{\phi}(u) \simeq h\phi'(0) = 2h\left(\sqrt{1 + b^2} - b\right) \tag{3.35}$$

Then we get:

$$\sigma_y^2 = \sigma_0^2 + \frac{2\pi^2 e^2 \tau \beta_y^2 h^2 \sigma_0^2 i^2}{\oint BE^2 \sigma_y^2 \sigma_x^2 \left(1+\frac{\sigma_y}{\sigma_x}\right)^2} \tag{3.36}$$

First of all we see here exactly the same formula (2.10) that was postulated in the work.[17] Comparing (3.36) with (2.10), we find

$$a = \frac{\pi e \beta_y h \sigma_0}{E \sigma_x \left(1 + \frac{\sigma_y}{\sigma_x}\right)} \sqrt{\frac{2\tau}{\oint B}} \tag{3.37}$$

An expression similar to (3.36) can also be found in the paper[44] (see Eq. (39) of this work) which gives to parameter h the physical meaning of the probability of finding the particle in a stochastic layer.

Expression (3.36) was also derived by J. Rees[56] from the assumption

$$\sigma_y^2 = \sigma_0^2 + \oint B \tau \beta_y^2 \theta_{rms}^2$$

where θ_{rms} is the effective r.m.s. scattering angle of a particle in the vertical plane, produced by the opposite bunch.

3.3.2 Scaling Laws

Expressions (3.36, 3.37) contain only one unknown parameter h. Let us consider it as a phenomenological parameter which should be determined from experimental data. One way to do this is to use PETRA results[17] (2.11). It is easy to see that to satisfy E^{-4} decrease for the value a, we need the following dependence of h on energy:

$$h \sim E^{-3/2} \tag{3.38}$$

Since we are interested now in maximum values of the luminosity and the current, we derive from (2.10) that asymptotically at large current i $\sigma_y^4 \simeq a^2 i^2$ or

$$\sigma_y \sim \frac{\sqrt{i}}{E^2} \tag{3.39}$$

The maximum possible value of σ_y limited by particle losses and beam lifetime should be some constant which can be written as $\sqrt{A_y \sigma_y}$ where A_y is an effective vertical acceptance of the storage ring. From formula (2.4) for Gaussian distribution we would find that σ_y is constant with the logarithmic accuracy. Let us see now what consequences follow from these assumptions.

a) Dependence on energy. Consider first the situation where the limitation arises from the beam lifetime. Assuming σ_y = const in expression (3.39) we immediately get

$$i_{max} \sim E^4 \tag{3.40}$$

With the help of this expression we also get the following scaling laws (note that for the electron storage ring $\sigma_x \sim E$):

$$\mathscr{L}_{max} \sim E^7 \tag{3.41}$$

$$\xi_{ymax} \sim E^2 \tag{3.42}$$

$$\xi_{xmax} \sim E \tag{3.43}$$

$$\frac{\sigma_y}{\sigma_x} \sim \frac{1}{E} \tag{3.44}$$

b) Dependence on current. Let us now turn to experiments in which beam lifetime limit has not been reached yet. At a given energy one gets from the same expressions:

$$\sigma_x\sigma_y \sim i^{1/2} \tag{3.45}$$

$$\xi_{ymax} \sim i^{1/2} \tag{3.46}$$

$$\mathscr{L}_{max} \sim i^{3/2} \tag{3.47}$$

c) Dependence on the number of bunches. For the strong-beam—weak-beam case we have observations made on ADONE.[21] Expression (3.36) in this case should be rewritten for the blowup of the weak beam by an unperturbed strong beam. Assuming the same dependence of h on E we have in this case

$$\sigma_y^2 \simeq \frac{i^2}{BE^{10}} \simeq \text{const} \tag{3.48}$$

The last equality corresponds to conditions of the ADONE experiment.[21] Hence,

$$i_{max} \sim E^5\sqrt{B} \tag{3.49}$$

$$\mathscr{L}_{max} \sim E^9 B \tag{3.50}$$

$$\xi_{ymax} \sim \frac{E^3}{\sqrt{B}} \tag{3.51}$$

$$\xi_{xmax} \sim \frac{E^2}{\sqrt{B}} \tag{3.52}$$

The scaling (3.49) seems to be in quite good agreement with the experimental data[21] on the strong-beam—weak-beam interaction at ADONE both

on E and on B. On the other hand, ξ_y and ξ_x were maintained equal. That makes the comparison of the energy dependence meaningless. The dependence on B is not contradictory to the experiment.

Tables 5 - 7 present the summary of the theoretical and experimental values for different parameters relevant for the beam-beam interaction. Keeping in mind the number of assumptions and the approximations made the agreement seems to be astonishingly good.

3.4 Computational Models

In this section I will discuss several simulations of the beam-beam interaction done on computers. All such simulations are performed by tracing a set of particles with different initial conditions through many interactions. Motion between the interactions is assumed to be linear (i.e., simple rotation in phase space with constant amplitude). Hence, the nonlinearities of the lattice are neglected.

The main attraction of the computational method for the investigation of the beam-beam phenomena (as well as many other complicated objects) is that this method presents a unique possibility to see the behavior of a sample of particles when the solution of the equations governing their motion is unknown. The finite capability of a computer forces us to neglect some features of the motion, thus making the method as approximate as any other. The approximation can be more or less physically sound, but it is always there. We see that the computational method is always applied to a certain physical model in the same way as the analytical method is. To some extent both methods can be considered as complimentary to each other since the analytical method is usually applicable only if there is a small parameter in the model.

The computational method usually exhibits a lot of troubles in the case of the presence of a small parameter.

There is also a substantial disadvantage in using the computational technique. It demands much skill to extract from the results of computations any general natural law— if it is possible at all. On the other hand, this method is sometimes the only one that is available.

Out of many simulations done,[37,47,57-61] I picked out rather arbitrarily only some done recently. I believe they quite substantially represent bright and dark sides of all computational efforts.

3.4.1 Tennyson's Model

The investigation of the weak-beam—strong-beam interaction in the electron storage ring is reported in work.[37] Two-dimensional motion is studied (that is no synchrotron oscillations are included). The following features of the motion are considered in both transverse planes:

a) linear transformation between interactions,

b) radiation damping of oscillations,

c) quantum fluctuations, and

d) the beam-beam interaction.

In the last, the vertical component of beam-beam force depends on the horizontal motion and is approximated by a Gaussian function in x. The dependence of the horizontal force on y has been omitted completely. In each run sixty-four different initial conditions, all corresponding to one standard deviation of the strong-beam in both planes were traced for the number of iterations corresponding to three damping times for each given energy of the particle.

First of all, the model exhibits blow-up in vertical direction and no significant change in horizontal size of the bunch. The blow-up occurs somewhere between the values of space charge, parameters ξ .02 and .06 and disappears if either radiation effects or beam-beam space charge parameter are put to zero in horizontal motion.

The effect does not depend on fluctuations in the vertical plane.

The blown-up beam shows a substantial tail of particles. Additional study of the cause of the blow-up discloses an interesting mechanism of rapid diffusion of a few particles along the resonance line. After such a particle reaches fairly large amplitude, it streams out of resonance and then is damped back to small amplitude.

The resonance particularly under suspision as being the main transporter of particles is

$$2\nu_x + 6\nu_y = 5 \quad .$$

The reason for such effectiveness by this resonance is that the resonance tube is almost along the A_y axis. Hence, small horizontal displacement (believed to be caused by quantum noise) can produce large vertical displacement.

3.4.2 Piwinski's Model

This model[60] also deals with the weak-beam—strong-beam interaction. All three degrees of freedom are considered here. Damping and quantum fluctuations of radiation are also taken into account.

Charge distribution of the strong-beam was assumed to be Gaussian. The "kicks" $\Delta x'$ and $\Delta y'$ are given in the integral form (1.4, 1.5). The integrals were tabulated for the grid of 75×200 points with the distances of $0.2\sigma_x$ and $0.2\sigma_y$ between them. Exact kick experienced by a

particle by the passage through the strong-beam was interpolated for each collision.

The tracking is performed for PETRA parameter $\sigma_x/\sigma_y = \beta_x/\beta_y = 15$, $\sigma_s/\beta_y = 0.1$, $\nu_x = 25.2$, $\nu_s = 0.07$ and different ν_y. Three different particle energies (7, 11.3, and 17.9 GeV) and three different numbers of bunches (1, 2 and 4) are studied. The initial coordinates of particles were uniformly distributed in phase and Gaussian in amplitude. The typical number of particles is 125. They were traced for up to twelve damping times.

Special attention is paid to possible asymmetries and distortions in the machine. In particular, differences of betatron phase advances between interaction points (including the change of this value due to synchrotron oscillation for a particle) and spurious horizontal dispersion function are investigated and show drastic influence on the beam blow-up. Small vertical dispersion at the interaction point as well as linear coupling of horizontal and vertical oscillations due to skew quadrupoles show no effect on the blow-up.

The results of simulation clearly demonstrate appearance of many additional resonances arising due to disturbances of the storage ring and synchrotron oscillations. The resonance augmentation of y_{rms} is seen even for the smallest space charge parameter studied ($\xi = 0.02$), and is pronounced stronger with increasing ξ to 0.06.

I think that observed influence of phase asymmetry strongly supports the hypothesis of a possible important role of machine nonlinearities in the beam-beam phenomena. Indeed, together with residual closed orbits, the nonlinearities can be responsible both for phase asymmetries and for additional resonances.

3.4.3 Talman's Model

This computational model[61] is the only one, as far as I know, which is designed to study the strong-beam—strong-beam effect. Many particles (~ 100 in each of the two beams) are tracked for many turns (~ 3000, which corresponds to approximately three damping times τ) in six-dimensional phase space. Radiation damping, quantum fluctuations and vertical coupling are taken into account.

For a period of 0.3τ one bunch is held rigid. From the tracking results for the particles of the second bunch, smooth distribution and the horizontal and vertical fields of this bunch is calculated. Then the roles of the two bunches are reversed.

The possibility of particle loss is incorporated by installing a mask (typically set at $\pm 10\sigma_x$ and $\pm 10\sigma_y$ for corresponding deviations). In this way the lifetime of the bunch can be found. For the conditions giving "good" lifetime, the luminosity is calculated from the equilibrium particle distributions. It is found that the regions of "bad" lifetime correlate with the positions of the resonances of the nonlinear equation of vertical motion parametrically "pumped" by the horizontal oscillations.

A comparison between the experimental observations and the results of computations shows good agreement both in the dependence of $\mathscr{L}(i)$ and in the values of i_{max} beyond which the lifetime is too short (see Fig. 3.2).

The sources of the beam blow-up as seen by the authors of all three computational studies are discerned quite differently. It is noise in the first,[37] machine distortions in the second[60] and strong coupling to horizontal motion in the third.[61] The same difference holds in respect

to a mechanism of the blow-up. It is a single resonance in the first, simultaneous action of many resonances in the second and parametric amplification of the vertical oscillations by horizontal in the third.

Such controversy is hardly surprising and might point to the existance of all three (and maybe even more) reasons for the beam instability.

CONCLUSION

Considering the state in which the beam-beam problem exists, what kind of feeling might one experience? Is it frustration or excitement? The answer is of course subjective.

Personally, I am more exhilarated — the physics with and of the storage ring is progressing rapidly after all — rather than disappointed with all the failures of proper description of the beam-beam phenomenon. We still have not been able to kill a bird, but it is a challenge to have it alive, too!

ACKNOWLEDGMENTS

This paper would never appear without the encouragement and advise of Dr. M. Month. I am also grateful to the organizers of this Workshop for the invitation to give this talk and to all the participants for their interest in it.

REFERENCES

1. Proceedings of the Beam-Beam Interaction Seminar, Stanford Linear Accelerator Center, Stanford, California, May 22-23, 1980; SLAC-PUB-2624.
2. Nonlinear Dynamics and the Beam-Beam Interaction, AIP Conference Proceedings, #57, eds. M. Month and J. Herrera, 1979.
3. F. Amman, IEEE Trans. NS-20, No. 3, 858 (1973).
4. H. Wiedeman, Ref. 2, p. 84.
5. A. Chao, Ref. 2, p. 42.
6. Y. Orlov, Sov. Phys. JETP, V. 5, No. 1, 45 (1957).
7. K. Robinson, CEA-54 (1958).
8. R. Sundelin, IEEE Trans. NS-26, No. 3, 3604 (1979); also, N. Vinokurov et al., Ref. 33, p. 254.
9. S. Kheifets, PETRA-KURMITTEILUNG N113 (1977).
10. A. Piwinski, Ref. 2, p. 115.
11. A. Piwinski, Proceedings of the 11th Interantional Conference on High Energy Accelerators, Geneva, 1980, p. 638.
12. Y. Derbenev, SLAC-Translation-151 (1973).
13. N. N. Chau, D. Potaux, Orsay, Rapport Technique 5-74 (1974).
14. N. N. Chau, D. Potaux, Orsay, Rapport Technique 2-75 (1975).
15. S. Kheifets, IEEE Trans. NS-26, No. 3, 3615 (1979).
16. S. Kheifets, M. Donald, P. Morton (unpublished).
17. G. Voss, "First and Only Partial Analysis of Space Charge Effects in Petra," DESY, M-VM-79/6 (1979).
18. D. Degèle et al., DESY 80/10 (1980); also, D. Degèle, Ref. 11, p. 16.
19. H. Zyngier, Ref. 2, p. 136.

20. J. LeDuff, Ref. 1, p. 80.

21. S. Tazzari, Ref. 2, p. 128.

22. M. Donald, J. Paterson, IEEE Trans. NS-26, No. 3, 3580 (1979).

23. M. Donald (private communication).

24. M. Sands, SLAC-121 (Nov. 1970).

25. H. Wiedemann (private communication).

26. G. Voss, Ref. 11, p. 748.

27. H. Wiedemann, Ref. 11, p. 744.

28. M. Cornaccia, Ref. 2, p. 99.

29. J. Paterson, Ref. 11, p. 7.

30. J. Rees (private communication).

31. P. Marin, Ref. 11, p. 742.

32. A. Hoffman, B. Zotter, Ref. 11, p. 713.

33. B. Zotter, Proceedings of the 10th International Conference on High Energy Accelerators, Serpukhov, 1977, Vol. II, p. 23.

34. M. Month, IEEE Trans. NS-22, 1376 (1975).

35. H. Hereward, CERN/ISR-DI/72-26 (1972).

36. J. LeDuff, CERN/ISR-AS/74-53 (1974).

37. J. Tennyson, Ref. 1, p.1.

38. A. Dragt, O. Jakubowicz, Ref. 1, p. 205.

39. J. Cary, LBL-6350 (1970).

40. A. Dragt, J. Finn, J. Appl. Math., Vol. 17, No. 12, 2215 (1976).

41. E. Keil, PEP-Note-59 (1973).

42. L. Teng, Ref. 1, p. 99.

43. S. Kheifets, Ref. 1, p. 40.

44. A. Ruggiero, "The Theory of Nonlinear Systems in Presence of Noise (the Beam-Beam Effect)," Fermilab (1980).

45. J. Greene, Ref. 1, p. 235.

46. T. Bountis, Ref. 1, p. 248.

47. C. Eminhizer, Ref. 1, p. 273.

48. B. Chirikov, Phys. Reports, 52, No. 5, 265 (1979).

49. E. Courant, Ref. 11, p. 763.

50. L. Teng, IEEE Trans. NS-20, No. 3, 843 (1973).

51. J. Greene, J. Math. Phys., 20, 1183 (1979).

52. F. Israilev, "Nearly Linear Mappings and Their Applications," (submitted for publication in Physica D, 1980).

53. P. Vuillermot, Ref. 1, p. 312.

54. T. Bountis, E. Coutsias, Ref. 2, p. 311.

55. R. Hellemann, Ref. 2, p. 236.

56. J. Rees (private communication).

57. E. Close, Ref. 2, p. 210.

58. J. Herrera, M. Month, R. Peierls, Ref. 2, p. 202.

59. D. Neuffer, A. Ruggiero, Ref. 1, p. 332.

60. A. Piwinski, Ref. 11, p. 754.

61. S. Peggs, R. Talman, Ref. 11, p. 754.

62. H. Uhm, C. Liu, Phys. Rev. Lett. 43, 914 (1979).

63. S. Kheifets, A. Chao, AATF/79/13, PEP-Note-325 (1979).

64. R. Hollebeek, Ref. 1, p. 165.

65. A. Garren, Ref. 11, p. 725.

66. R. Sah, Ref. 11, p. 736.

67. A. Chao, E. Keil, A. King, M. Lee, P. Morton, J. Peterson, SPEAR-187,(1975).

68. A. Wrulich, Int. Ber. DESY, PET-77/03,(1977).

69. F. Amman, D. Ritson, International Conference on High Energy Accelerators, Brookhaven, 1961, p. 471.

70. E. Courant, IEEE Trans. NS-12, No. 3, 550 (1965).

71. D. Ritson, J. Rees, SLAC-TN-65-39 (1965).

72. M. Bassetti, 5th International Conference on High Energy Accelerators, Frascati, 1965, p. 708.

73. The CESR Operations Group, Ref. 11, p. 26.

74. The VEPP-4 Group, Ref. 11, p. 38.

TABLE I

Dependence of SPEAR parameters on the particle energy E, in GeV. The fit is done[27] by a function $f = kE^q$.

f	k	q	Comment
$\mathscr{L}_{max}$	0.033	6.6	in 10^{30} cm^{-2} sec^{-1}
i_{max}	1.2	3.6	in ma
$\frac{\sigma_y}{\sigma_x}$	0.5	-1.0	-
ξ_x	0.022	0.87	-
ξ_y	0.011	2.3	-

TABLE II

Dependence of SPEAR parameters on the beam current i, in ma. The fit is done by a function $f = ki^q$.

f	E [a]	k	q	β_y	Comment
$\mathscr{L}_{max}$ [b]	1.5 2.5 3.7	0.030 0.046 0.054	1.95 1.55 1.45		high energy physics runs
$\mathscr{L}_{max}$ [b]	1.95 1.95	0.052	1.41 1.45	10 cm 20 cm	machine physics runs
σ_y σ_x ξ_y	 2.4	 	0.59 0 0.33	 	

[a] in GeV.

[b] 10^{30} cm^{-2} sec^{-1}

TABLE III

Dependence of ADONE parameters on the particle energy E, in GeV.[21] The fit is done by a function $f = kE^q$.

f	k	q	Comment
$\mathscr{L}_{max}$	0.64	7	in 10^{30} cm^{-2} sec^{-1}
$\xi_x \simeq \xi_y$	0.068	1.57	-
i_{max} (in ma)	105	4.34	three bunches } Strong-Beam-Weak-Beam
	42.4	4.12	one bunch } Strong-Beam-Weak-Beam

TABLE IV

Some Experimental Observations

Machines	E (GeV)	Vertical Tune	β_y (cm)	B	Scaling Laws/E				ξ_{max} (10^{-2})
					I (E)	$\mathscr{L}$ (E)	S*(E)	ξ (E)	
ACO	.54	.829	400	1-2	$\gamma^{3.5}$	γ^{5}	γ^{2}	$\gamma^{0.5}$	3.1
VEPP-2M	.65	3.086	5.6	1		$\gamma^{4}-\gamma^{6}$			2.6 [a]
VEPP-4	1.84	9.1	15.0			γ^{4}			1.5
ADONE	1.5	3.05	340	3	$\gamma^{4.5}$	γ^{7}	γ^{2}	$\gamma^{1.5}$	6.6
DCI	1.85	1.79	200	1	γ^{1}	γ^{2}	γ^{0}	γ^{0}	4.1
DORIS	5.0	5.18	30	360	γ^{3}	γ^{4}	γ^{2}	γ^{0}	1.0
SPEAR	2.0	5.17	10	1	$\gamma^{3.6}$	$\gamma^{6.7}$		$\gamma^{2.4}$	4.5

[a] In the case of VEPP-2M, these data are extracted from a contribution to the 1978 Dubna Conference.

TABLE V

The power q in the power law $f(E) \sim E^q$.

Parameter	Experiment			Model	Equation	Comment
	SPEAR	ADONE	PETRA			
h				$-\frac{3}{2}$	3.38	
$\mathscr{L}_{max}$	6.6	7		7	3.41	
i_{max}	3.6	4.5		4	3.40	Strong-Strong
i_{max}		4.12 4.34		5	3.49	Weak-Strong
ξ_y	2.3	1.5		2	3.42	
ξ_x	0.9			1	3.43	
$\frac{\sigma_y}{\sigma_x}$	-1			-1	3.44	
a			-4	-4	2.11	

TABLE VI

The power q in the power law $f(i) \sim i^q$

Parameter	Experiment			Model	Equation
	SPEAR	ADONE	PETRA		
$\mathscr{L}_{max}$	1.4			1.5	3.47
$\mathscr{L}_{spmax}$			-0.5	-0.5	
$\sigma_x\sigma_y$	0.6			0.5	3.45
ξ_y	0.4			0.5	3.46

TABLE VII

The power q in the power law $f(B) \sim B^q$.

Parameter	Experiment			Model	Equation	Comment
	SPEAR	ADONE	PETRA			
i_{max}		0.8		0.5	3.49	Strong-Beam — Weak-Beam
ξ_{ymax}		-0.8		-0.5	3.51	

FIGURE CAPTIONS

Fig. 1.1 Horizontal kick $\Delta x'$ (in mrad) as a function of vertical displacement y in units of vertical dispersion b of the opposite Gaussian bunch. The calculations[9] are done for PETRA parameters (current per bunch I_b = 20 ma, round beam, p = 1).

Fig. 1.2 Vertical kick $\Delta y'$ (in mrad) for the same conditions as Fig. 1.1.

Fig. 1.3 Horizontal kick x' (in mrad) as a function of horizontal displacement x/a. Elliptical beam with aspect ratio p = 0.25. All other parameters the same as in Fig. 1.1.

Fig. 1.4 Horizontal kick $\Delta x'$ as a function of vertical displacement y/b (see caption to Fig. 1.3).

Fig. 1.5 Vertical kick $\Delta y'$ as a function of horizontal displacement x/a (see caption to Fig. 1.3).

Fig. 1.6 Vertical kick $\Delta y'$ as a function of vertical displacement y/b (see caption to Fig. 1.3).

Fig. 1.7 Resonances in vertical motion due to beam-beam interaction. Results of computer simulation for DORIS storage ring.[10] The ratio of the maximum to the minimum betatron amplitude is shown. Only those resonances are shown for which the amplitude increase exceeds 50%.

Fig. 1.8 Stability region of the dipole coherent oscillations for 1×1 bunch collision.[5] The picture repeats itself with the period $\Delta\nu = 0.5$. ν on abscissa is 1/2 of the actual machine tune.

Fig. 1.9 Stability region of the dipole coherent oscillations for 3×3 bunches collision.[5] The limit space charge parameter ξ_{limit} is plotted versus ν which is actually the number of vertical betatron oscillations for 1/6 of the ring (the distance between the next two interaction points).

Fig. 1.10 Resonance web for higher modes of coherent betatron oscillations.[14] The shaded areas around the resonance lines show the widths of the resonance due to beam-beam interaction.

The space charge parameter $\xi = 0.05$. Only the resonances are shown, the widths of which are greater than 10^{-3}. One can see that the largest available working zones are located along the difference coupling resonance $\nu_x = \nu_y$.

Fig. 1.11 Beam blow-up in the weak-strong case as measured on SPEAR.[15] The solid line represents calculations according to diffusion phenomenological model (see Section 3.2 and expression 3.33 for the parameter η used as abscissa).

Fig. 1.12 Vertical beam profile measurements on SPEAR.[16] Curves correspond to the following conditions:

N	Bunch	I_+(ma)	I_-(ma)	Condition
1	electron	1.70	6.8	Beams are Separated
2	electron	1.70	6.8	Beams Collide
3	positron	1.75	6.9	Beams Collide
4	positron	1.75	7.0	Beams are Separated

Fig. 1.13 Beam blow-up for the strong-strong case. The density distribution is measured[4] with the help of scrapers by observing the reduction of beam lifetime as a function of the scraper position y. For a Gaussian bunch the value y/σ_y calculated from the beam lifetime (see expression 2.4) would be a linear function of y.

Fig. 1.14 Operation zones found[19] on the storage rings ACO (a) and DCI (b).

Fig. 2.1 Results of luminosity measurements[30] on PEP for two collision modes 1×1 and 3×3 bunches. The deviation from I^2 law starts for 1×1 mode at bunch current $\simeq 4$ ma, while for 3×3 mode there is no threshold.

Fig. 2.2 Specific luminosity $\left(\mathscr{L}_{sp} = \mathscr{L}/BI_B^2\right)$ for PEP.[30]

Fig. 2.3 Space charge parameter ξ_y (tune shift) for PEP.[30]

Fig. 3.1. Schematic behavior of tune shift and resonance width as functions of particle amplitude (out of work[5]).

Fig. 3.2. Comparison of the experimental observations at CESR and the results of computation according to Talman's model[61].

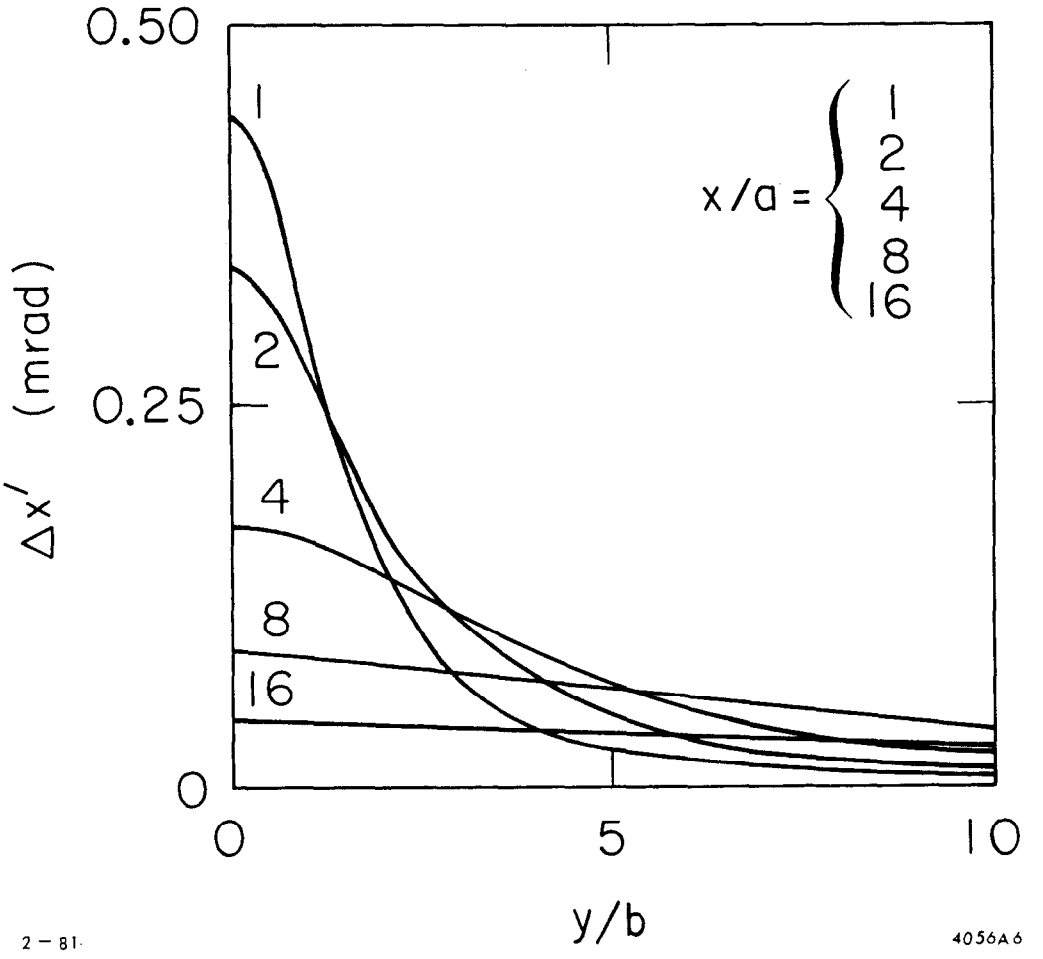

Fig. 1.1

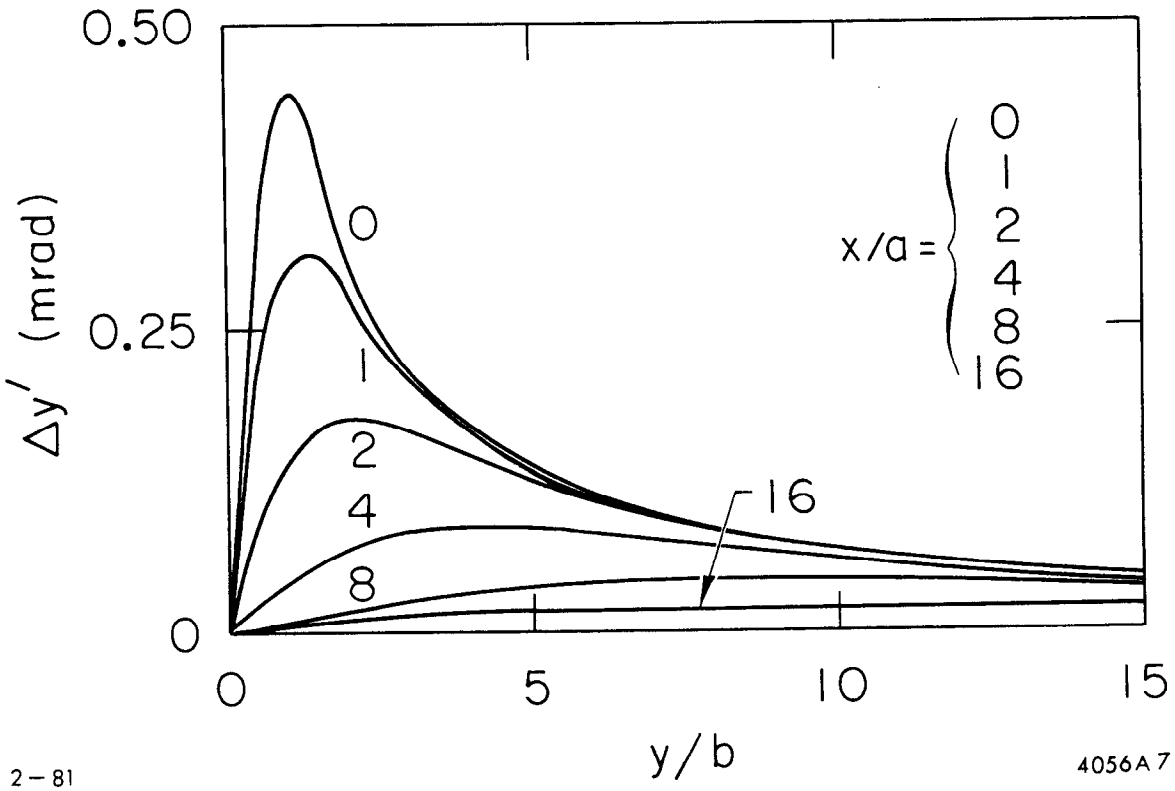

Fig. 1.2

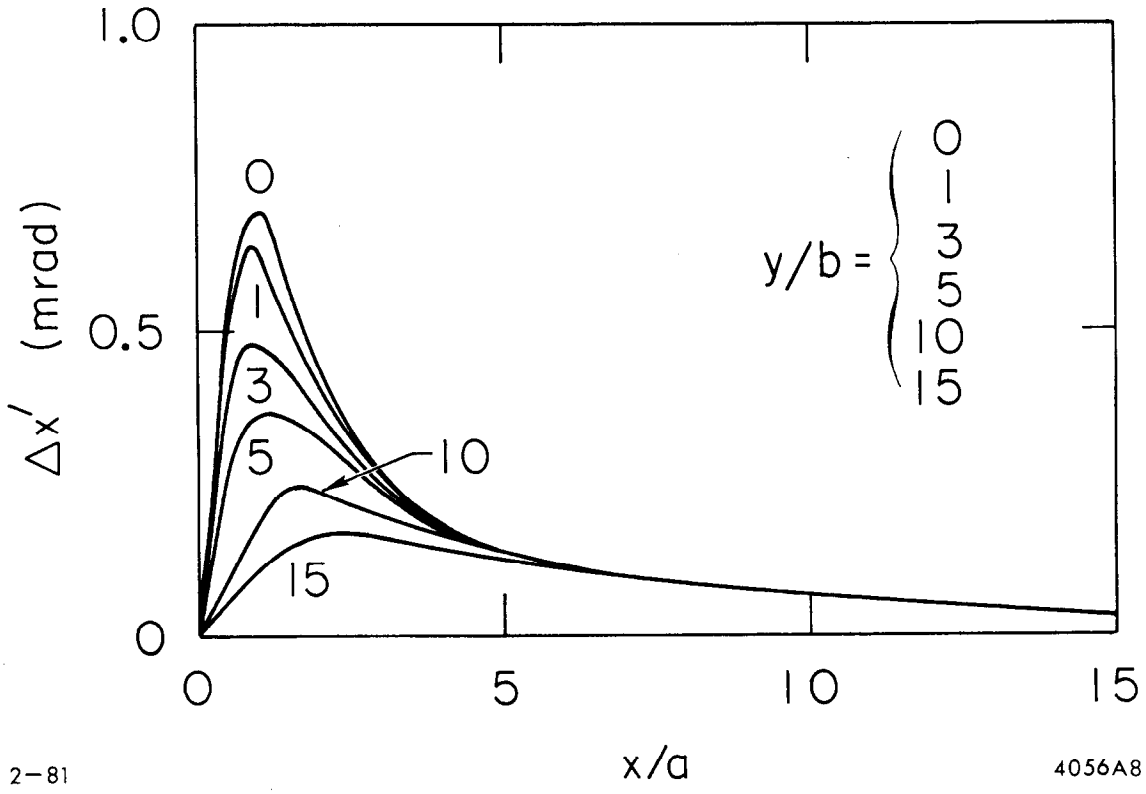

Fig. 1.3

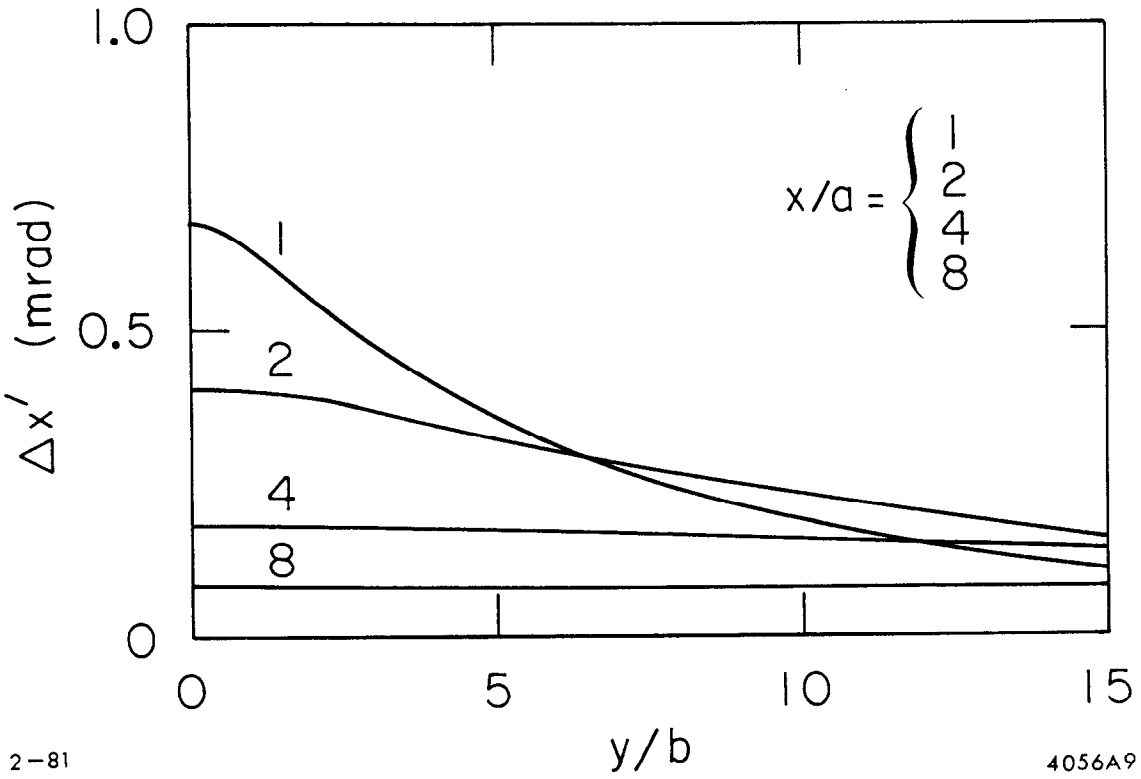

Fig. 1.4

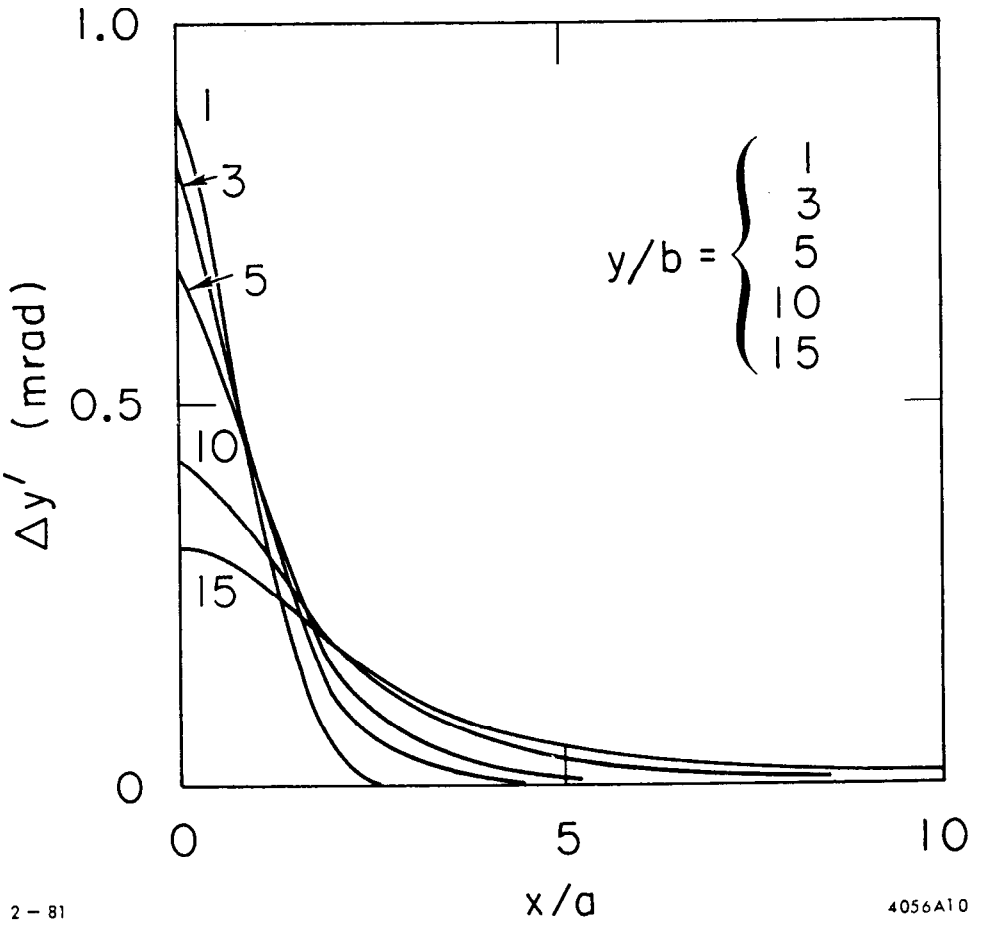

Fig. 1.5

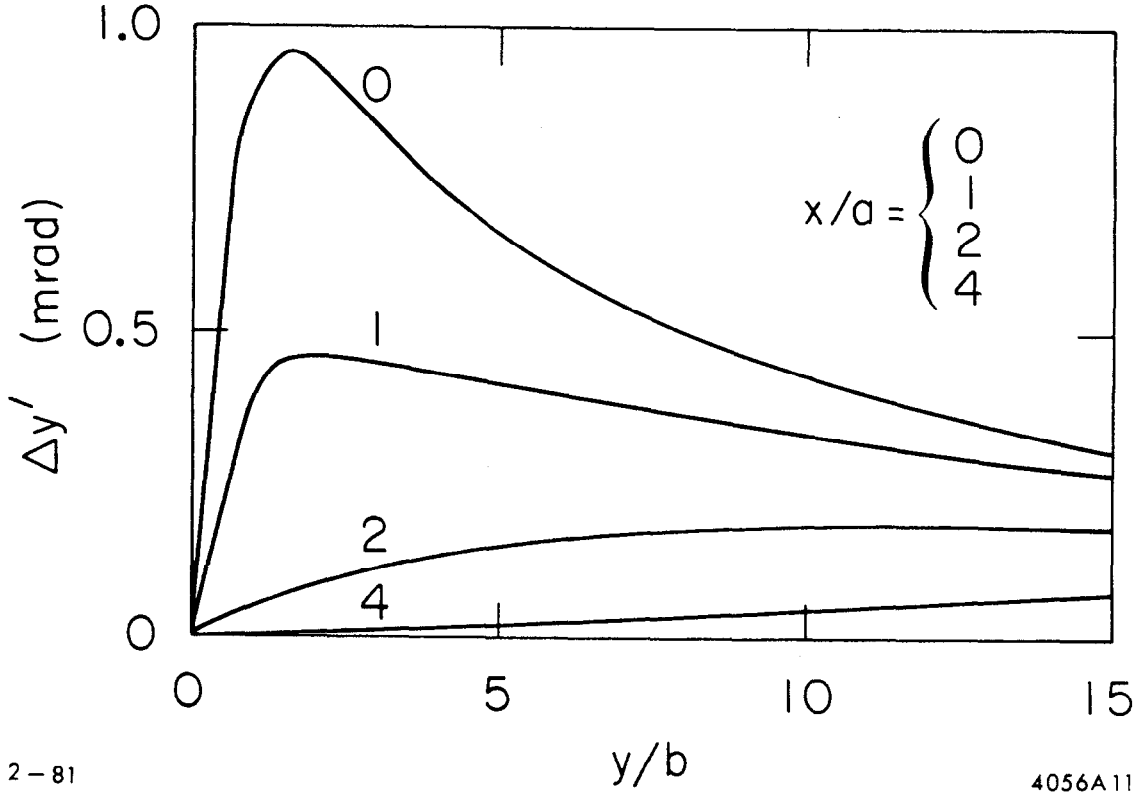

Fig. 1.6

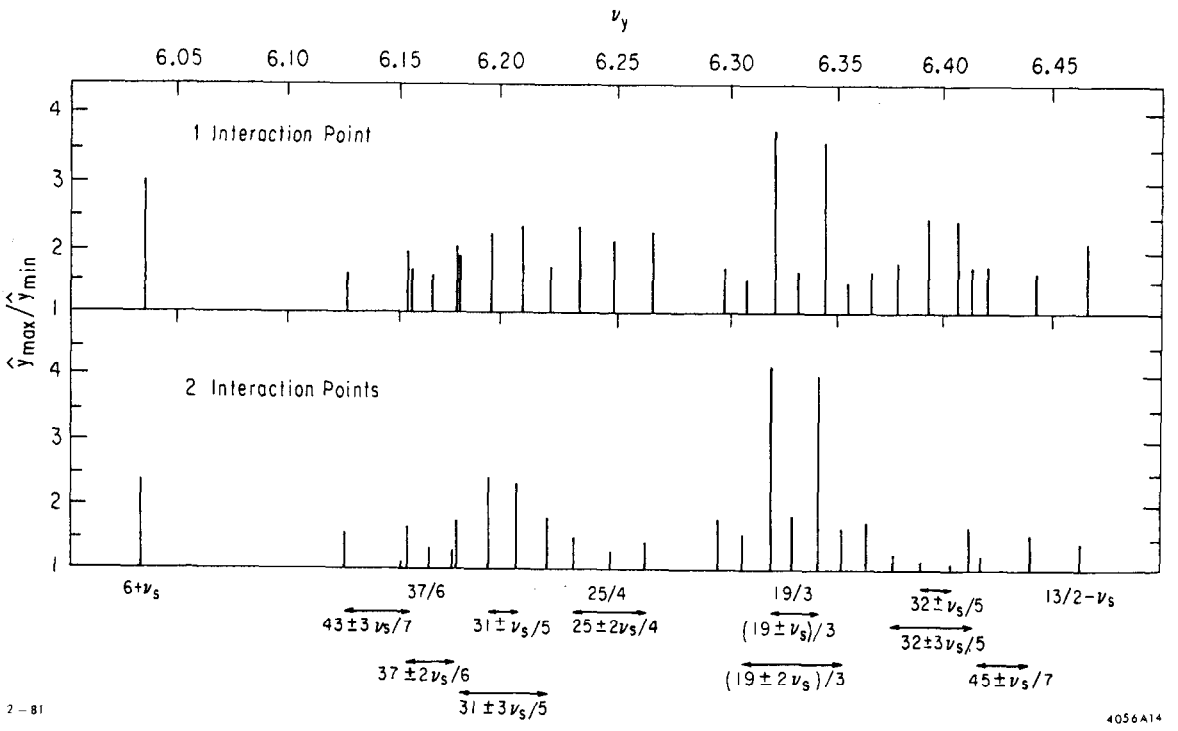
ν_y
6.05
6.10
6.15
6.20
6.25
6.30
6.35
6.40
6.45
1 Interaction Point
2 Interaction Points
$\hat{y}_{max}/\hat{y}_{min}$
1
2
3
4
$6+\nu_s$
37/6
$43\pm3\nu_s/7$
$37\pm2\nu_s/6$
$31\pm3\nu_s/5$
$31\pm\nu_s/5$
25/4
$25\pm2\nu_s/4$
19/3
$(19\pm\nu_s)/3$
$(19\pm2\nu_s)/3$
$32\pm\nu_s/5$
$32\pm3\nu_s/5$
$45\pm\nu_s/7$
$13/2-\nu_s$
2-81
4056A14

Fig. 1.7

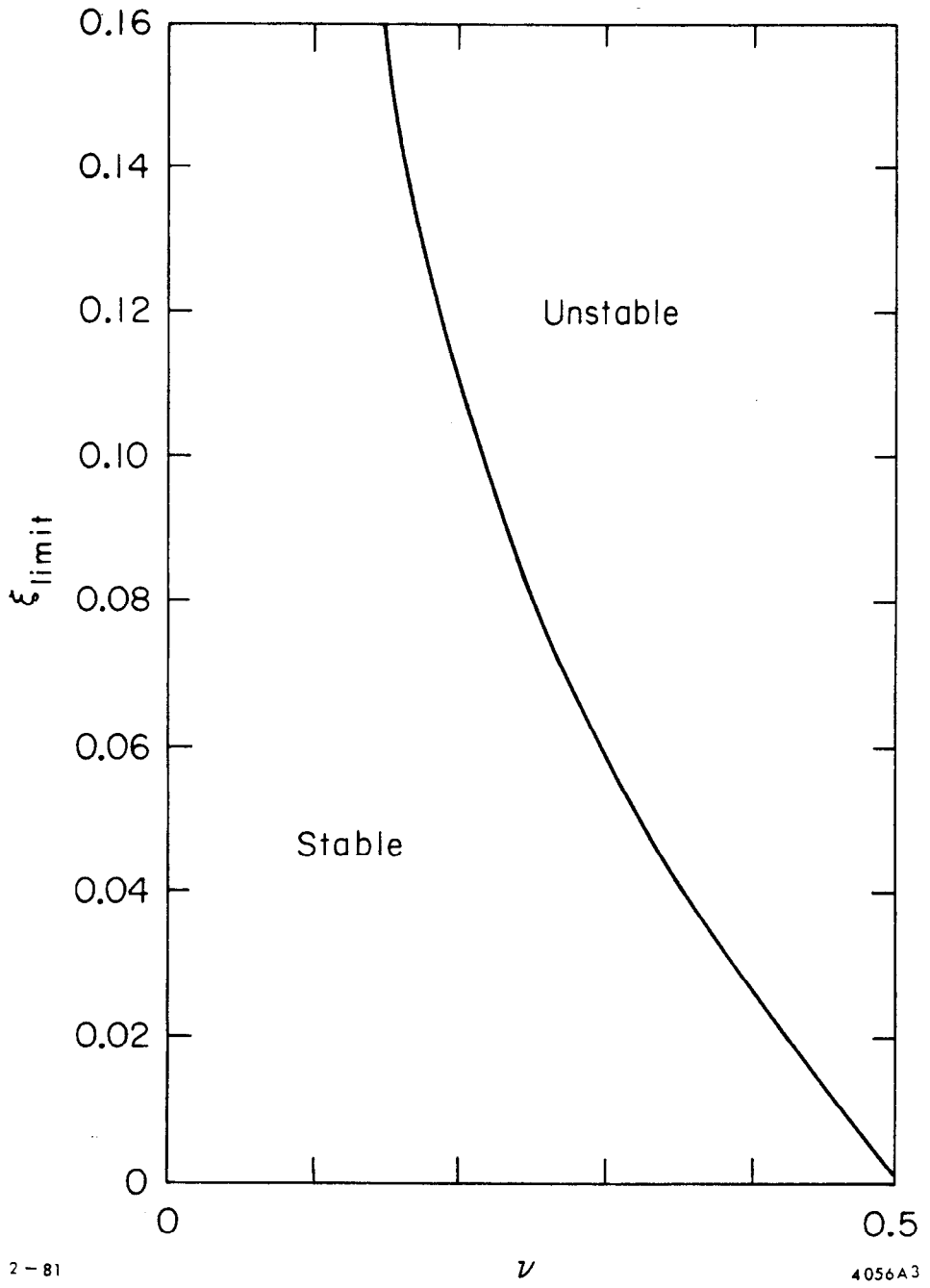
0.16
0.14
0.12
0.10
0.08
0.06
0.04
0.02
0
ξ_{limit}
Unstable
Stable
0
0.5
ν
2-81
4056A3

Fig. 1.8

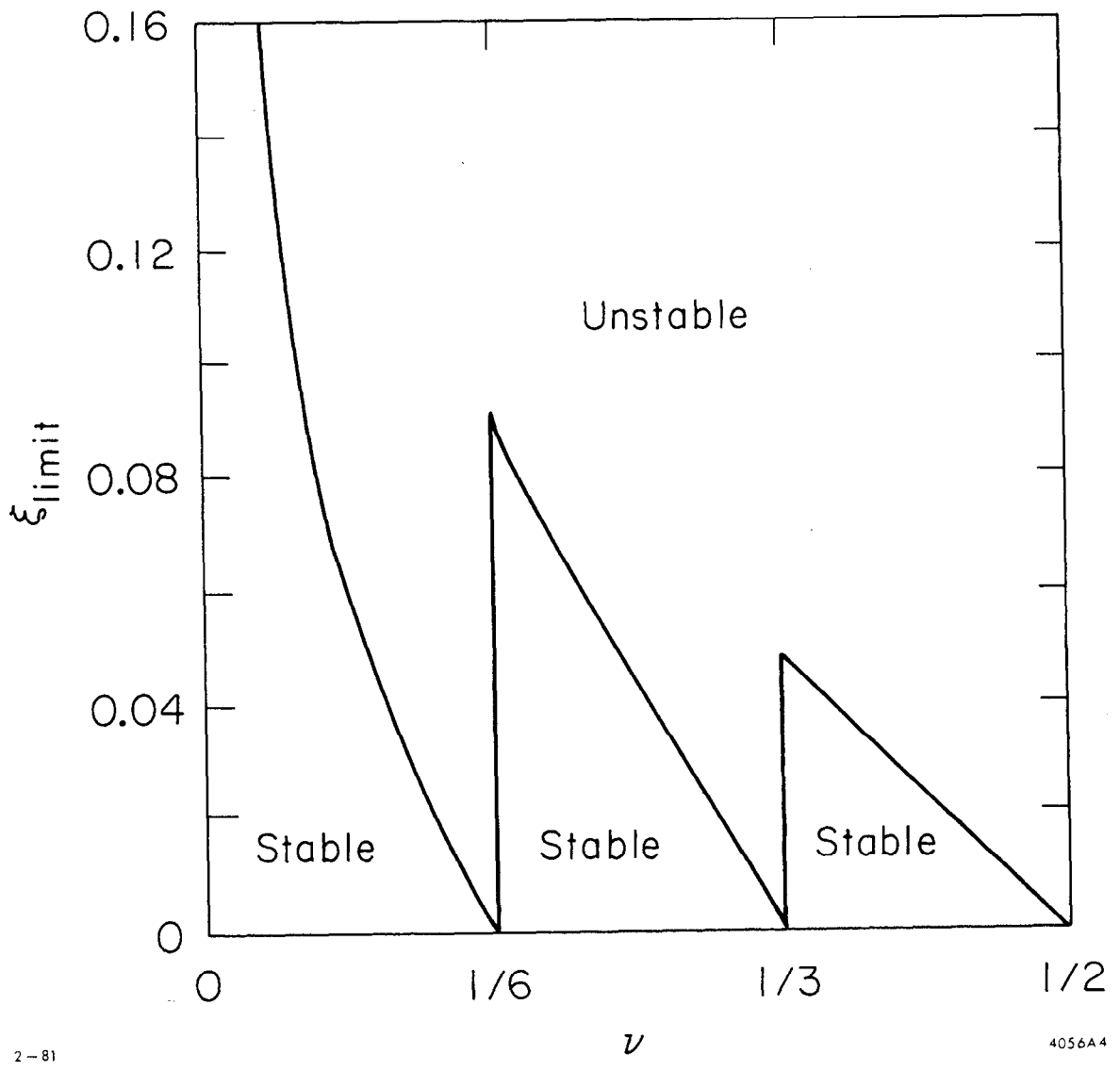
0.16
0.12
0.08
0.04
0
ξ_{limit}
Unstable
Stable
Stable
Stable
0
1/6
1/3
1/2
ν
2-81
4056A4

Fig. 1.9

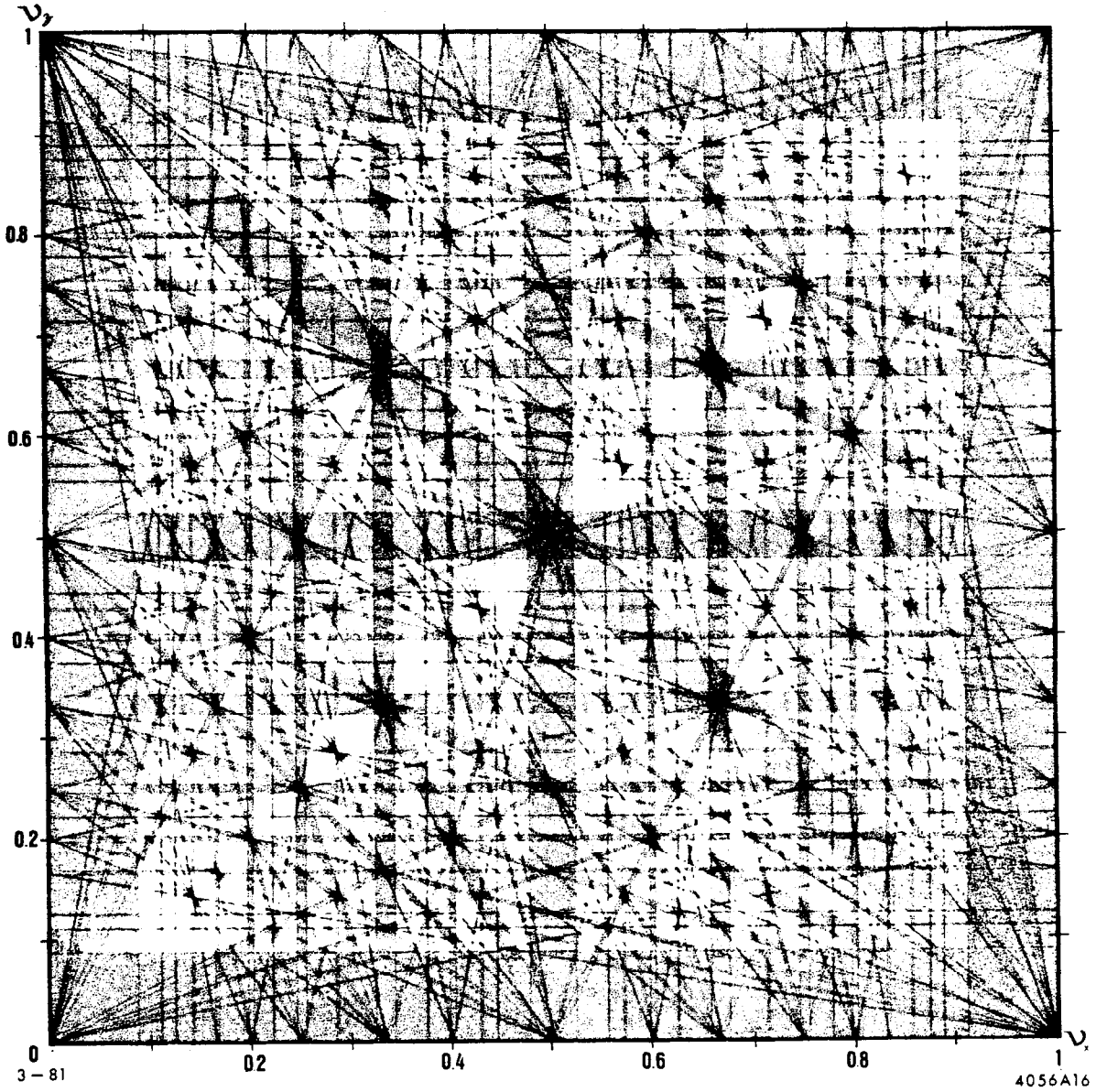

Fig. 1.10

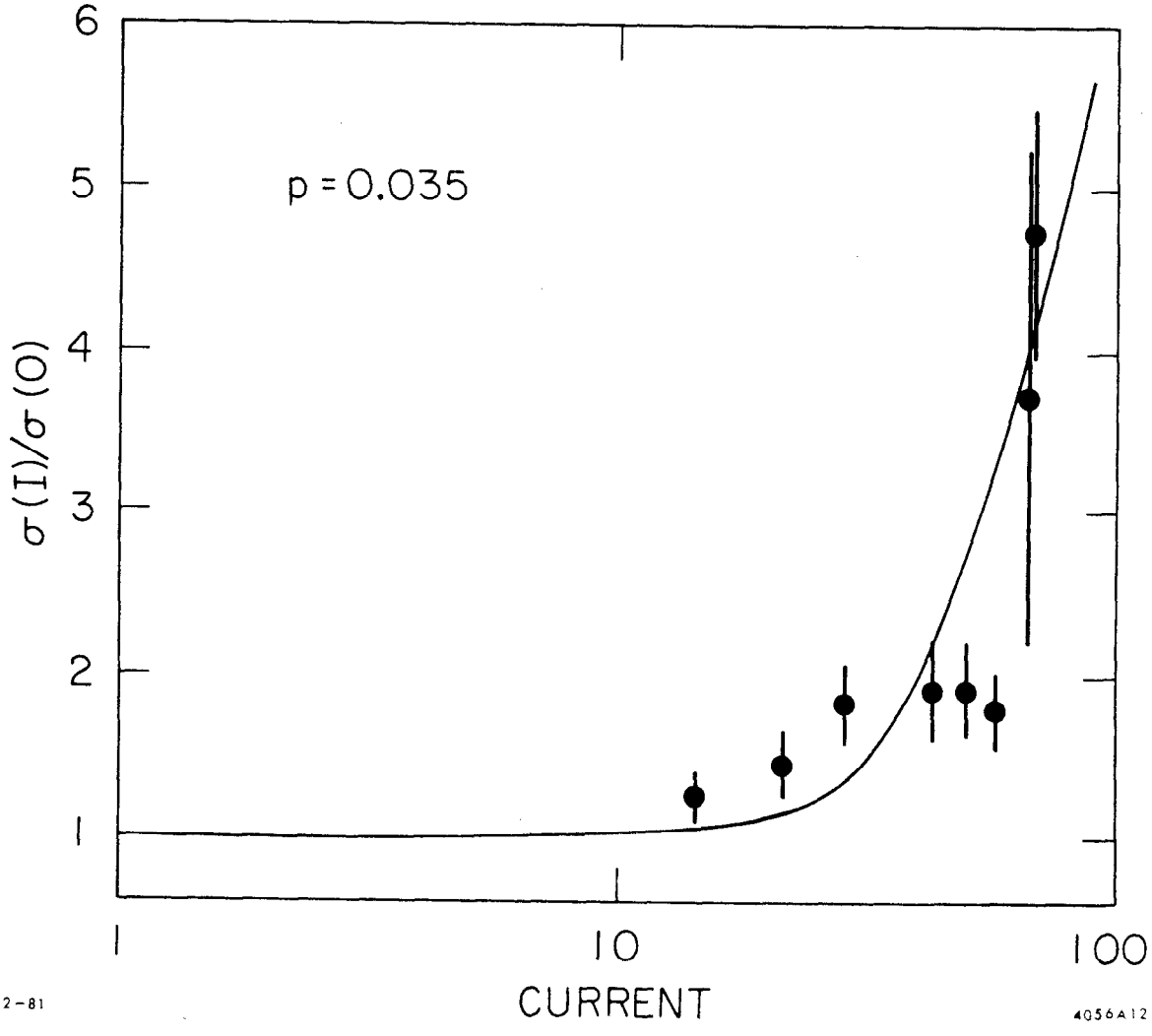

Fig. 1.11

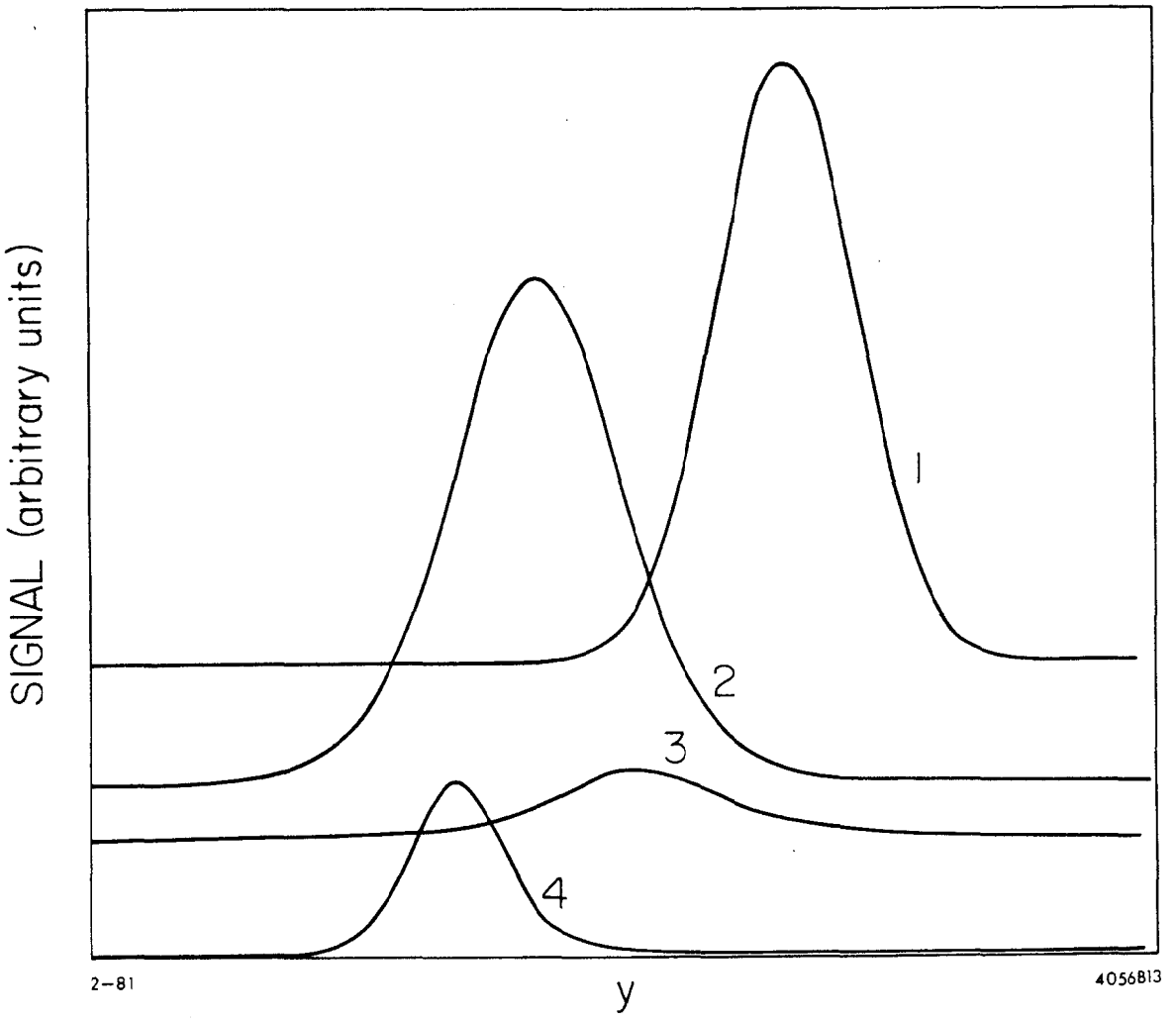

Fig. 1.12

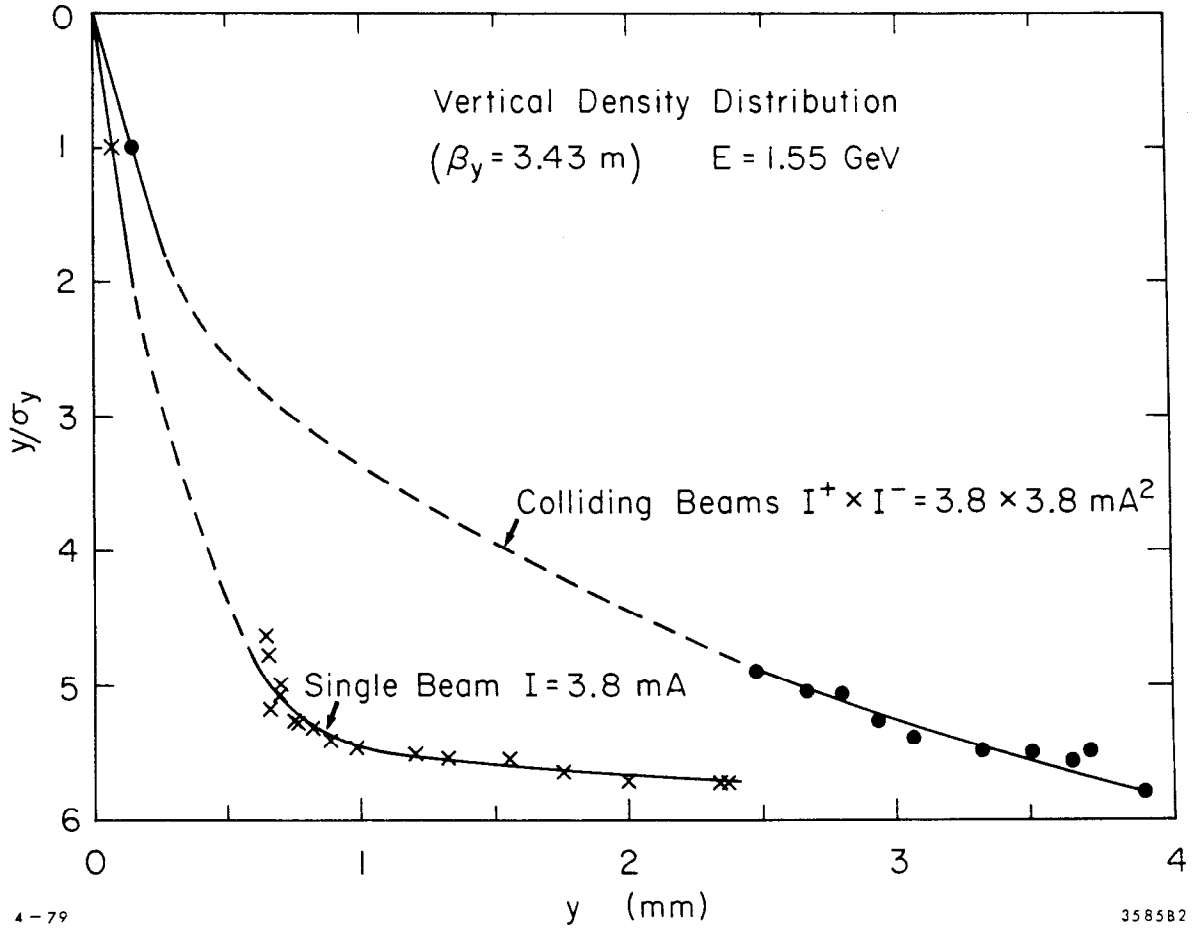
Vertical Density Distribution
(β_y = 3.43 m) E = 1.55 GeV
Colliding Beams $I^+ \times I^- = 3.8 \times 3.8$ mA^2
Single Beam I = 3.8 mA
y/σ_y
y (mm)
0
1
2
3
4
5
6
4-79
3585B2

Fig. 1.13

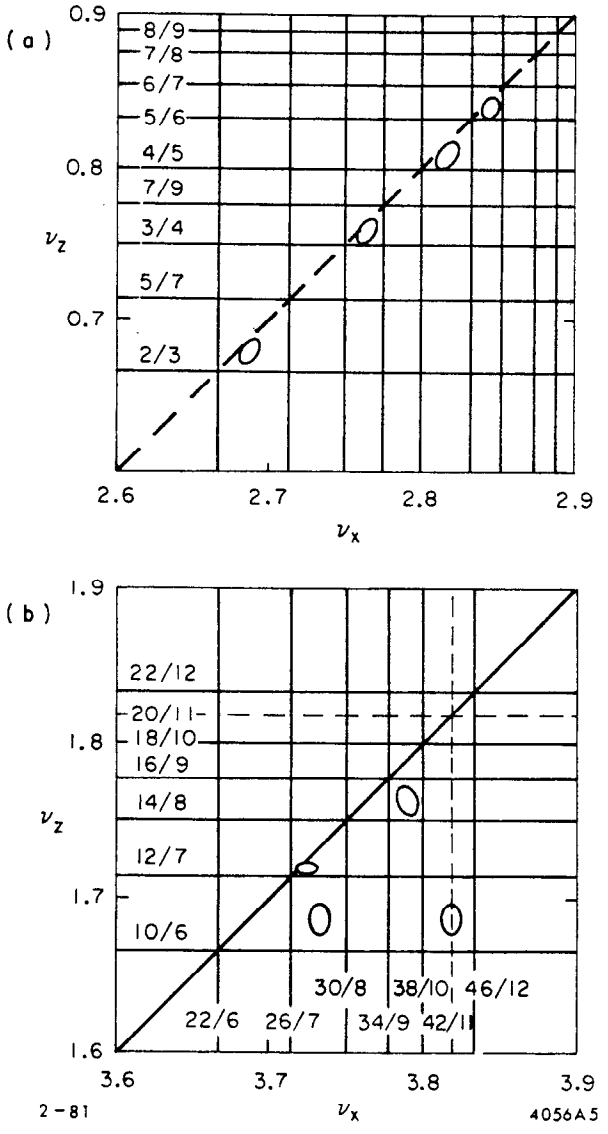
(a)
0.9
8/9
7/8
6/7
5/6
4/5
0.8
7/9
3/4
ν_z
5/7
0.7
2/3
2.6
2.7
2.8
2.9
ν_x
(b)
1.9
22/12
20/11
1.8
18/10
16/9
14/8
ν_z
12/7
1.7
10/6
30/8
38/10
46/12
22/6
26/7
34/9
42/11
1.6
3.6
3.7
3.8
3.9
ν_x
2-81
4056A5

Fig. 1.14

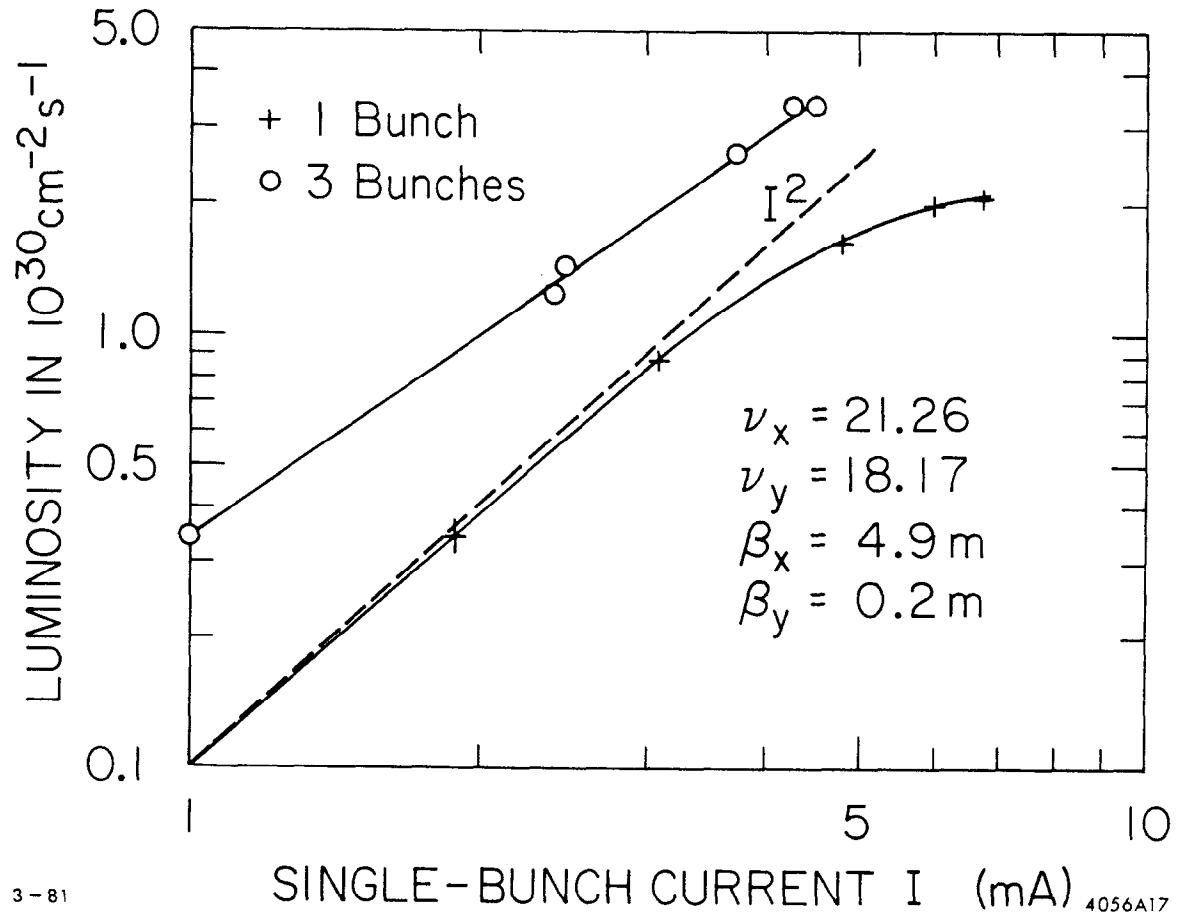
5.0
1.0
0.5
0.1
LUMINOSITY IN $10^{30}cm^{-2}s^{-1}$
+ 1 Bunch
o 3 Bunches
I^2
$\nu_x = 21.26$
$\nu_y = 18.17$
$\beta_x = 4.9\,m$
$\beta_y = 0.2\,m$
1
5
10
SINGLE-BUNCH CURRENT I (mA)
3-81
4056A17

Fig. 2.1

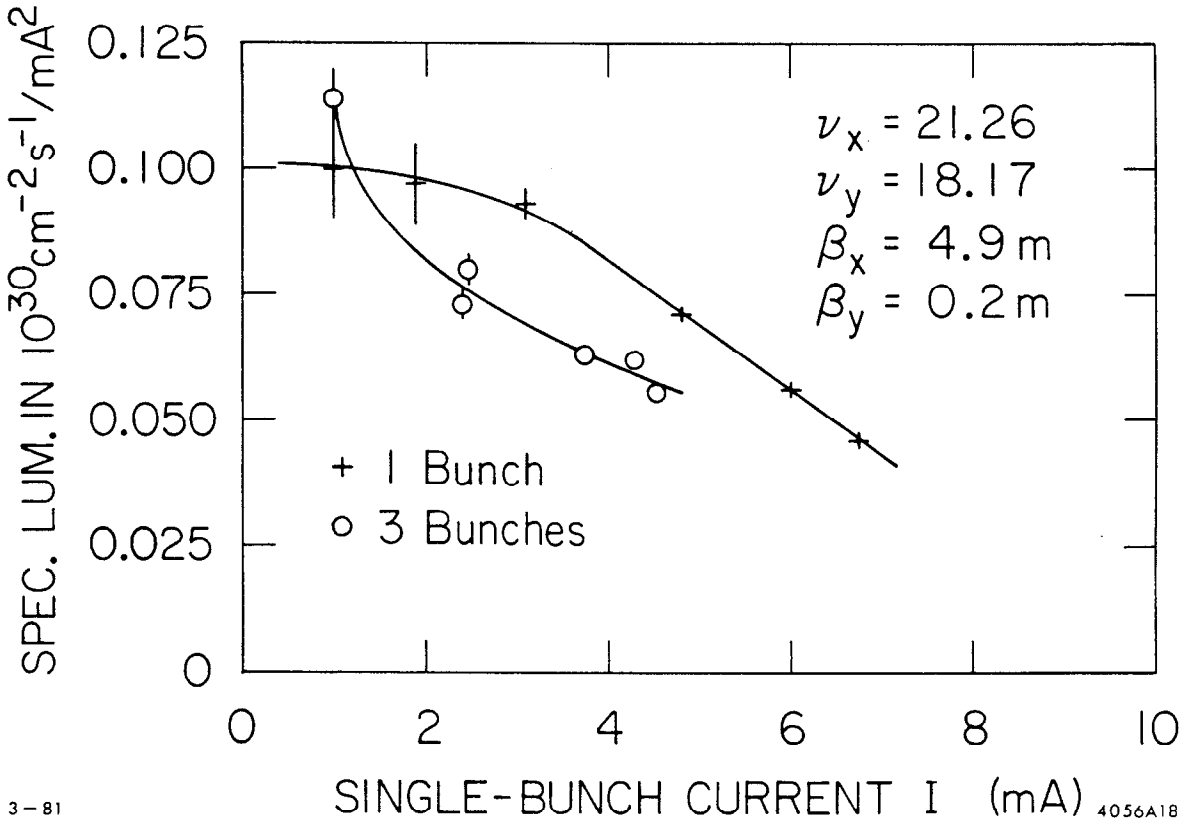
SPEC. LUM. IN $10^{30}cm^{-2}s^{-1}/mA^2$
0.125
0.100
0.075
0.050
0.025
0
0
2
4
6
8
10
SINGLE-BUNCH CURRENT I (mA)
ν_x = 21.26
ν_y = 18.17
β_x = 4.9 m
β_y = 0.2 m
+ 1 Bunch
o 3 Bunches
3-81
4056A18

Fig. 2.2

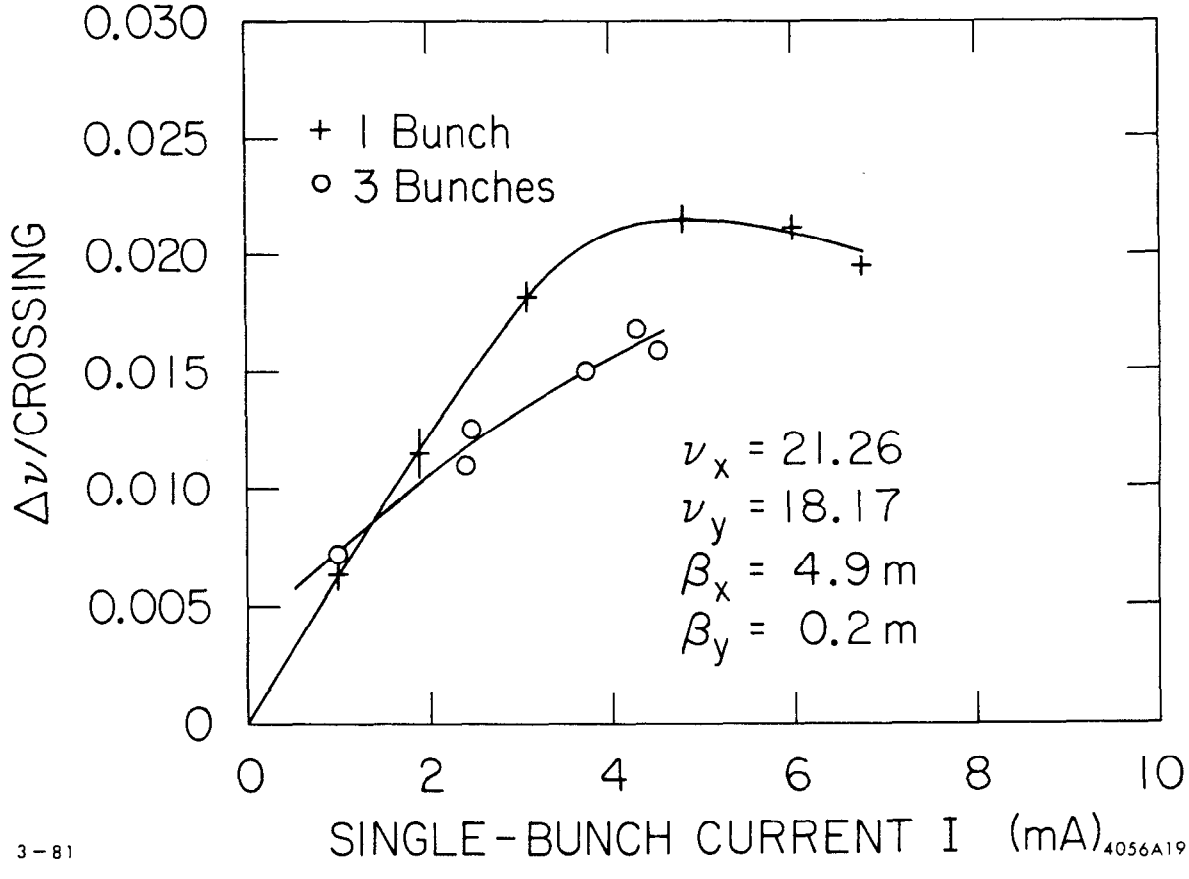
0.030
0.025
0.020
0.015
0.010
0.005
0
Δν/CROSSING
+ 1 Bunch
o 3 Bunches
ν_x = 21.26
ν_y = 18.17
β_x = 4.9 m
β_y = 0.2 m
0
2
4
6
8
10
SINGLE-BUNCH CURRENT I (mA)
3-81
4056A19

Fig. 2.3

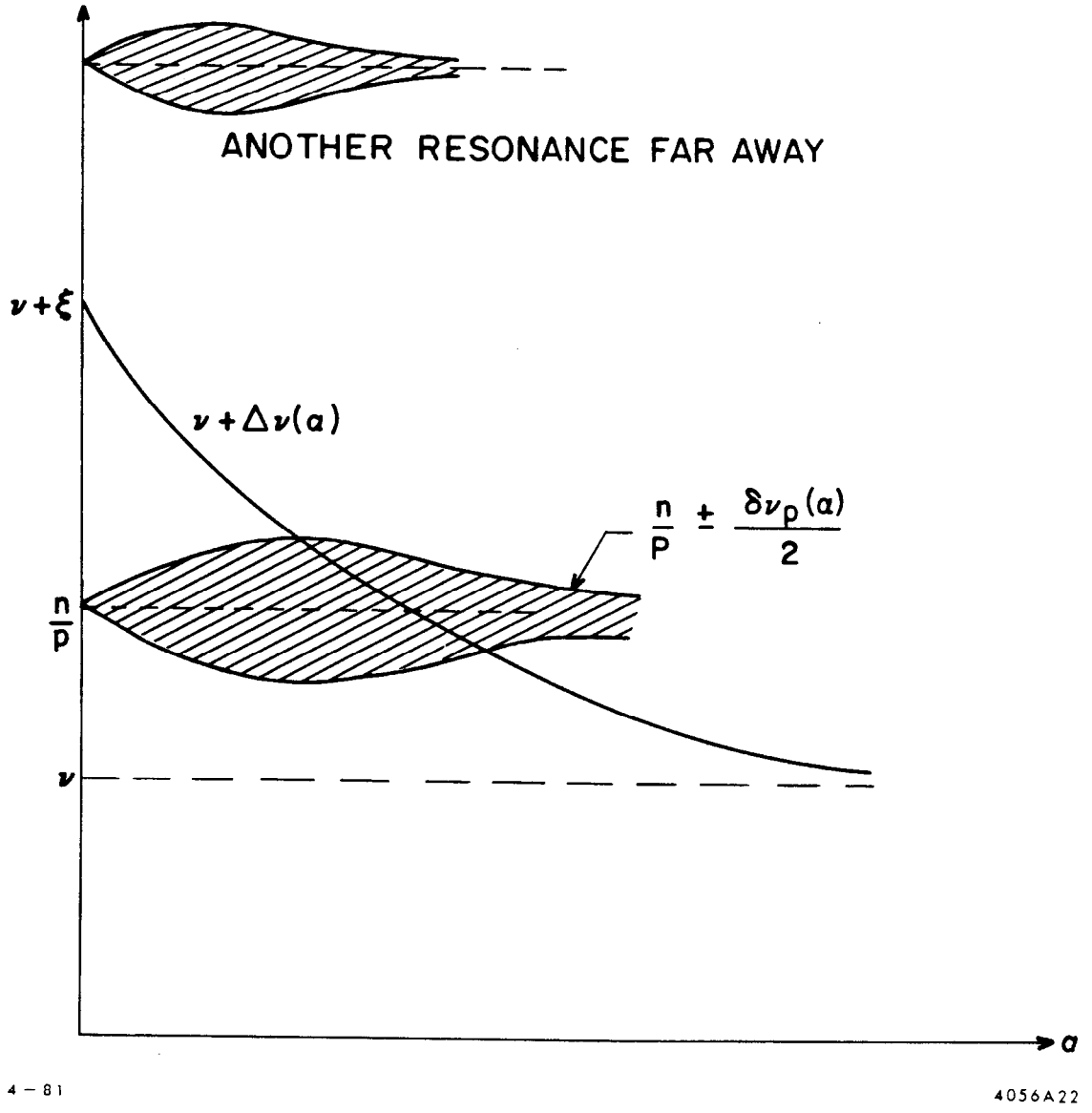
ANOTHER RESONANCE FAR AWAY
$\nu+\xi$
$\nu+\Delta\nu(a)$
$\frac{n}{P} \pm \frac{\delta\nu_p(a)}{2}$
$\frac{n}{p}$
ν
a
4 – 81
4056A22

Fig. 3.1

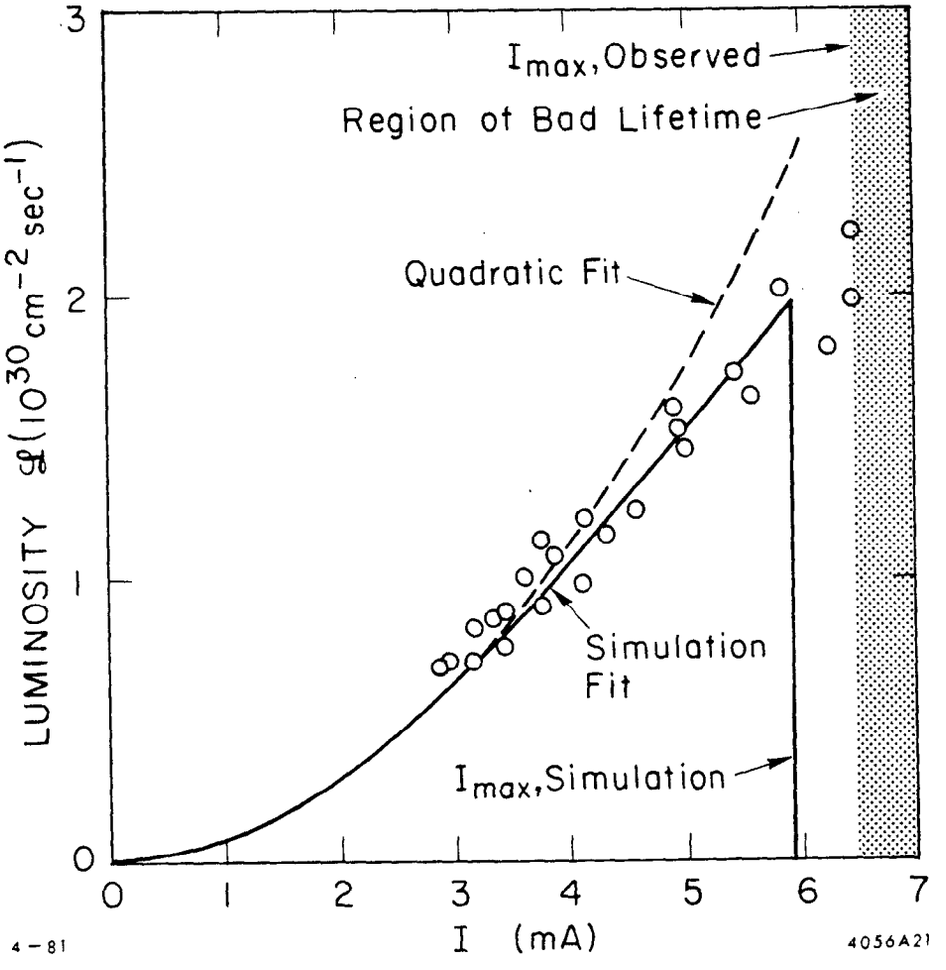
I_{max}, Observed
Region of Bad Lifetime
Quadratic Fit
Simulation Fit
I_{max}, Simulation
LUMINOSITY $\mathcal{L}(10^{30} cm^{-2} sec^{-1})$
I (mA)
0
1
2
3
4
5
6
7
4-81
4056A21

Fig. 3.2